UNIVERSITY OF CALIFORNIA, MERCED

Activation of the NLRP3 inflammasome by Chlamydia infection

by

Ye Zhu

A dissertation submitted in partial satisfaction of the requirements for the degree Doctor of Philosophy

in

Quantitative and System Biology

Committee in charge:
Professor Nestor Oviedo, Chair
Professor Patricia LiWang
Professor Wei-Chun Chin

Spring 2016

The dissertation of Ye Zhu is approved:

Nestor Oviedo, Chair Date

Patricia LiWang Date

Wei-Chun Chin Date

David M. Ojcius, Instructor Date

University of California, Merced

DEDICATION

To my parents Zhaoliang Zhu and Jun Li

and

my families

For

their endless love and supports!

TABLE OF CONTENTS

LIST OF ABBREVIATIONS

BMDM	Bone marrow derived macrophages
cDNA	Complementary DNA
CLR	C-type lectin receptor
C.pn	Chlamydia pneumoniae
C.pi	Chlamydia psittaci
C.t	Chlamydia trachomatis
DAMPs	Danger associated molecular patterns
DC	Dendritic cells
EBs	Elementary bodies
ELISA	Enzyme-linked immunosorbent assay
GAPDH	Glyceraldehyde 3-phosphate dehydrogenase
HeLa	Human cervical carcinoma cell line
IFN	Interferon
IKK	IκB kinase
IL	Interleukin
IL-1Rs	Interleukin-1 receptors
IRAK	IL-1 receptor-associated kinase
IRF-7	Interferon regulatory factor 7
IκB	Inhibitor of NF-κB
KO	Knockout
LPS	Lipopolysaccharide

LRR	Leucine-rich-repeat
MEFs	Mouse embryonic fibroblasts
MOI	Multiplicity of infection
MOMP	Major outer membrane protein
MoPn	Mouse pneumoniti (*Chlamydia muridarum*)
mRNA	Messenger RNA
NF-κB	Nuclear factor-kabba B
NLRs	NOD-like receptors
NOD	Nucleotide-binding oligomerization domain
PAMPs	Pathogen-associated molecular patterns
PRR	Pathogen Recognition Receptors
Q-PCR	Quantitative polymerase chain reaction
RBs	Reticulate bodies
RIG-I	Retinoic acid inducible gene-I
RLRs	RIG-I-like receptors
RT	Reverse transcription
SD	Standard deviation
STD	Sexual transmitted diseases
shRNA	Short hairpin RNA
Th1	T helper-1 cells
THP1	Human acute monocytic leukemia cell line
TIR	Toll/IL-1R domain

TRAF6	TNF-receptor-associated factor 6
WT	Wild Type

LIST OF FIGURES

LIST OF TABLES

ACKNOWLEDGMENTS

First of all, I would like to sincerely thank my advisor Professor David M. Ojcius. This project would not have been possible without his constant guidance over the years. I was inspired and enlightened by his profound knowledge, acute insights, deep understanding of the philosophy of research, sense of humor and most importantly, meticulous attention to details.

I would like to thank my dissertation committee - Professors Nestor Oviedo and Patricia LiWang from the School of Natural Science, and Professor Wei-Chun Chin from the School of Engineering - for their timely, insightful comments and constructive guidance that significantly improved this dissertation.

I would also like to express my gratitude to Kathleen Kelly and Janina Jiang from the Department of Pathology and Lab Medicine in UCLA. I appreciate their help on the vaults project. Also a big thanks to Tamer Alpagot for the IRB application and the patients' samples collection for the pneumonia project. Many thanks go to my previous and current laboratory colleagues at UC Merced and UOP.

The financial support from the National Institute of Health Foundation Grant NIH grant AI079004 is gratefully acknowledged. I would also like to thank the numerous fellowship awards from UC Merced, financial support and training from the research and teaching assistants at UC Merced.

Last but not least I would like to express my sincere gratitude to my parents and friends. With their endless support and love, I will always keep a positive attitude and a sense of responsibility.

Curriculum Vitae

- Ph.D. in Quantitative and System Biology. University of California, Merced (UCM). Merced, CA, USA. Aug. 2011-May 2016
- B.S. in Biotechnology. Beijing Institute of Technology (BIT). Beijing, China. Sept. 2004-July 2008

Publications

- Ye Zhu[1], Hongbin Wang[1], Hailong Wang [1], Xiao Wang[2]*,Yulin Deng[1]*.Quantitive proteomics analysis of biological effect of proton radiation on SHSY5Y cells. BCEIA.2009
- Zhu, Y., Champion, C., Said-Sadier, N., Boxx, G., Jiang, J., Tetlow, A., Kickhoefer,V., Rome, L.H., Ojcius, D.M., Kelly, K.A. Activation of the NLRP3 inflammasome by vault nanoparticles. Vaccine,2013.
- Syed Qasim Raza [1-4], **Ye Zhu[12]**, et al. Entescence, a non-cell-autonomous senescence program initiated by cellular cannibalism. *Cell*. Reviewing. (2016)

Conference

- Poster presentation in the ISHCI 13th (Jun.2014)
- Poster presentation in the CBRS 2013 (Mar.2013)
- Presentation in the Chlamydia Group Seminar with UCLA/UC Irvine/UC Davis (Feb.2013)
- Attended BAMPS conference in UCSF (Mar.2012)

Honors

- 2012 Graduate Student Fellowship
- 2012 Summer Fellowship
- 2013 Summer Fellowship
- 2014 Summer Fellowship
- 2015 Summer Fellowship

Abstract

Activation of the NLRP3 inflammasome by Chlamydia infection

by

Ye Zhu

Doctor of Philosophy

in

School of Natural Science

University of California, Merced

Professor David M. Ojcius, Instructor

Professor Nestor Oviedo, Chair

Spring 2016

The inflammasome is a multi-protein complex that serves as the first line of immune defense. NLRP3 is one of the most widely studied inflammasomes, which can be activated by a wide range of stimuli including membrane-damaging toxins, pathogen associated molecular patterns (PAMPs), and danger associated molecular patterns (DAMPs). Chlamydia is a genus of small, Gram-negative, obligate intracellular bacteria comprising four species. Among them, *Chlamydia trachomatis* (*C.t*) is the leading cause of bacterial sexual transmitted diseases (STD) worldwide, for which there are currently no effective vaccines. This is due to the difficulties in identifying and delivering relevant T cell antigens and in developing appropriate adjuvants. Vaults are large, cylindrical cytoplasmic ribonucleoprotein particles found in nearly all eukaryotic cells. Recombinant vaults that encapsulate chlamydia epitopes are highly stable structures *in vitro*, therefore could be employed as an ideal vaccine vehicle for epitope delivery. In the first part of this

study, we tested the ability of vaults containing an immunogenic chlamydial epitope of *C. trachomatis* to be internalized into human monocytes and to activate the NLRP3 inflammasome. We demonstrate that chlamydia vaults co-localized with lysosomes and cathepsin B release is required for the NLRP3 inflammasome activation. Our data show that chlamydia vaults also involve in the non-canonical inflammasome and are important for inflammasome activation.

Chlamydia pneumoniae (C.pn) is an airborne chlamydial species responsible for human respiratory infection. *C.pn* persists within the infected tissues for periods in order to stimulate a chronic inflammatory response. The inflammation activated by *C.pn* is known to play an important role in the pathogenesis of atherosclerosis. *C.pn* has been shown to disseminate systemically from the lungs through infected peripheral blood mononuclear cells and to localize in arteries where it may infect endothelial cells, vascular smooth muscle cells, monocytes/ macrophages and promote inflammatory atherogenous process. Importantly, *C.pn* has recently been shown to be a new member of the human oral microbiota. It appears to be related to some oral infectious diseases including caries, periodontitis, endodonit infections, and tonsillitis. However, whether *C.pn* infects oral cells and induces cellular responses remains unknown. Therefore, we hypothesize that *C.pn* infects oral epithelial cells and activates the NLRP3 inflammasome. In the second part of this study, we provided evidence that *C.pn* infection activates the NLRP3 inflammasome in GECs and induces IL-1β and caspase-1 secretion. Interestingly, we also found that *C.pn* is frequently present in plaques from patients with periodontitis, indicating a potential correlation of periodontitis with respiratory infection or atherosclerosis.

Chapter 1 Introduction

1. Innate Immunology

1.1 Pattern Recognition Receptor

Humans are exposed to millions of potential pathogens every day. The immune system protects the human body from numerous pathogenic microbes at the site of infection. To get rid of the infections, the human body relies on both innate immunity and also adaptive immunity. The innate immune response consists of cells and molecules that are always present and are ready to impede and kill the microbes at the infection site. The adaptive immune response functions against the microbes that are able to evade the innate immune response. While adaptive immunity is specific to particular pathogens and is capable of creating immunological memory, innate immunity recognizes conserved features of pathogens and rapidly activates the inflammasome.

The initial sensing of infection is mediated by the germline-encoded pattern recognition receptors (PRR), including Toll-like receptors (TLRs), NOD-like receptors, RIG-I-like receptors and C-type lectin receptors. These PRRs detect conserved structures among microorganisms, which are classified in two types: pathogen-associated molecular patterns (PAMPs) and damage-associated molecular patterns (DAMPs) [1-3]. PAMPs are molecules that associate with pathogens, represent pathogens, and bind with PRRs present at the cell surface or intracellular to activate downstream signaling pathway [4]. Bacterial lipopolysaccharides (LPS), endotoxins from bacteria cell membranes, flagellin, pepitidoglycan and nucleic acid from bacteria are all considered as PAMPs. PAMPs are derived from pathogens, while DAMPs are cell derived. DAMPs are also described as danger signals, when these molecules or signals are present in aberrant locations or abnormal molecular complexes that result from cell stress or tissue damages[2, 5].

Well-studied PRRs are the toll like receptors (TLRs). TLRs are first described as toll, which is a receptor identified in the fruit fly *Drosophila melanogaster*. So far there are ten TLRs identified so far in human and thirteen in mice, and TLRs from 1 to 9 are common for both [6-8]. TLR contains N-terminal leucine-rich repeats (LRRs), a trans-membrane region and the cytoplasmic Toll/IL-1R homology (TIR) domain. The extracellular LRRs are responsible for sensing and recognizing pathogens and then mediating ligand binding in the downstream signaling. Once activated, most TLRs dimerized and the TIR domains recruit intracellular/cytosol signaling adaptors TIRAP (Myd88 adaptor)[8].In the downstream adaptor, MyD88 associates with IRAK-1 and/or IRAK-2 and activates IRAK-4. IRAK-4 recruits and phosphorylates the IRAK1/2 complex transiently, which will further attract the (TNF)-receptor-associated factor 6

(TRAF6). TRAF6 in turn polyubiquinates the protein TAK1 and TAK1 then phosphorylates the inhibitor of NF-κB (IκB) kinase (IKK) [9, 10]. As a result, NF-κB is activated and translocated into the nucleus and ultimately up-regulates the transcription of proinflammatory cytokines like IL-1β and IL-6, which are associated with inflammation and cell survival.

1.2 The NOD Like Receptor

The nucleotide-binding oligomerizeation domain (NOD) like receptors (NLRs) is another widely studied RPP, which are intracellular sensors of PAMPs and DAMPs. NRLs are intracellular sensors for PAMPs and DAMPs and are generally made up of three parts: an N-terminal effector domain, a shared domain architecture including a nucleotide-binding domain (NBD), and a leucine rich repeat (LRRs) domain [11-13]. Similar to TLRs, the LRRs domain of NLRs detect the conserved microbial patterns (PAMPs/DAMPs) and then modulate NLR activities like rearrangements and oligomerization [13]. The N-terminal effector domain is responsible for protein-protein interaction including the caspase-recruitment domain (CARD), pyrin domain (PYD). To date, there are 22 NLR genes found in the human genome and 34 in the mouse [14]. NLRs are highly conserved through evolution. Their homologs have been discovered in many different animal species (APAF1) [15, 16]. According to their N-terminal domains, NLR could be classified into four subfamilies: the NLRP subfamily which expressing pyrin domains (PYDs), the CARDs subfamily containing NODs, the baculoyiral inhibitor of apoptosis repeat (BIR) subfamily, and the transactivator domain (AD) subfamily [17].

NLRs usually cooperate with TLRs and regulate the innate immune response. We described TLR activation as the first signal, which activates the NF-κB activation and up-regulates the transcription of pro-inflammatory chemokines/cytokines such as IL-1β. However, the up-regulated pro- IL-1β synthesis is not sufficient to induce IL-1β activation. A second signal is needed to boost IL-1β activation via NLRs. Once NLRs senses the dangerous signal, they will recruit some downstream adaptors constructed as a protein complex to further activate pro-caspase-1and IL-1β. We named this protein complex the inflammasome. Therefore, both the first and second signals are required to induce IL-1β secretion [18, 19].

1.3 Inflammasome

The inflammasome is a multi-protein complex that contains NLRs and adaptors like caspase-1. Inflammasomes serve as the first line of immune defense against inducers of cellular stress [20]. Following detection of stress inducers such as infection, inflammasomes promote maturation and secretion of IL-1β [21].

Inflammasomes are often defined by their PRR family member, which will behave as a scaffold protein that recruits caspase-1 proteins together and induces caspase-1 activation at the same time. Inflammasomes such as the NLRP3 inflammasome, RIG-I inflammasome and AIM2 inflammasome are mostly found in the antiviral immunity. The NLRP3 inflammasome is one of the well-studied inflammasomes and can be activated by a wide range of stimuli, including membrane-damaging toxins, PAMPs and DAMPs [22-25]. The NLRP3 inflammasome can also be stimulated by large particles such as monosodium urate (MSU) crystals, silica, nanoparticles, and the adjuvant, alum, which can lead to lysosomal damage after engulfment by phagocytes and the release of lysosomal proteases such as cathepsin B [26-28]. When these stimuli are detected, NLRP3 interacts with the adaptor, ASC (Apoptosis-associated speck-like protein containing a CARD), which in turn recruits the protease, pro-caspase-1. When pro-caspase-1 is assembled into the inflammasome, it becomes auto-activated and cleaves into a 20 KD fragment and induces caspase-1-dependent maturation and secretion of proinflammatory cytokines such as IL-1β [24, 29-33]. Upon activation of the NLRP3 inflammasome, the mature IL-1β is secreted out of the cells. In many cells such as monocytes and macrophages, the activated 20 KD form of caspase-1 is also secreted.

Spleen tyrosine kinase (Syk) has also been considered a key regulator when coupled to the NLRP3 inflammasome during fungal infection and Chlamydia trachomatis infection. Phosphorylation of Syk is believed to regulate the entry of *chlamydia* into host cells in lipid raft domains. This is probably because lipid rafts have been observed to participate with the formation of phagosomes involving Syk recruitment [34-36].

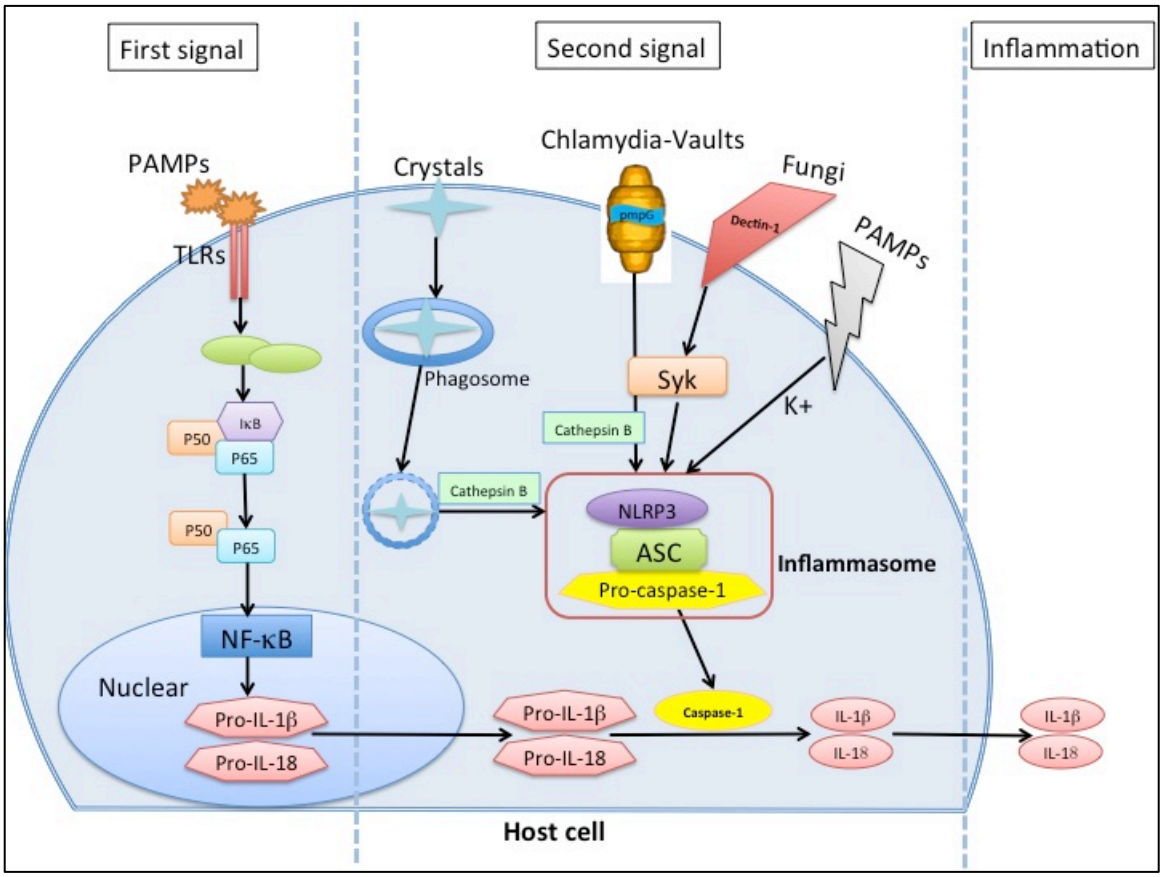

Figure 1. NLRP3-mediated caspase-1 activation requires two signals.

1.4 Non-canonical inflammasome

To date, two types of inflammasomes have been classified: canonical and non-canonical inflammasomes. In the past decades, four different inflammasomes, namely NLRP1, NLRP3, NLRC4 and AIM2 have been identified and characterized. The four NLRs represent the canonical inflammasome pathway and are all dependent on caspase-1 mediated activation. However, a recent study showed that the pathways leading to caspase-1 activation in response to microbial signals might be more complex than previously thought. The caspase-11 in mice and caspase-4/5 in human also play an alternative mechanism for caspase-1 activation [37-39]. Therefore the conception of non-canonical is given, as an alternative mechanism for caspase-1 activation.

2. Chlamydial strains

2.1 Chlamydia trachomatis

Chlamydia is used as a model system because its' species represent the world's leading cause of preventable blindness, and is a common cause of respiratory and sexually-transmitted infections in humans. There are three pathogenic chlamydial species found in the human body: *Chlamydia trachomatis, Chlamydia pneumoniae* and *Chlamydia psittaci.*

Chlamydia trachomatis (*C.t*) is the most prevalent bacterial sexually transmitted disease (STD) in the United States. Over 90 million new cases occur annually. *C.t* infections in women can cause pelvic inflammatory disease (PID) and result in infertility, ectopic pregnancy, and chronic pelvic pain [40]. Most *C.t* infections are asymptomatic, which makes it hard for women to be diagnosed, increasing the risk of transmission and spread of the infection [41, 42].

Identification of protective responses is a key component for vaccine development. Intensive studies have been done in order to dissect immunity towards to resolution of primary chlamydial infection, and immunity to reinfection in mouse genital infection model. CD4+ T cells play major role in resolving primary genital infection [43], particularly IFN-γ secreting CD4+ T cells (Th1 cells) [44], with or without CD8+ T cells or antibody [45, 46]. CD4+ T cells and/or antibody are also essential for resistance to reinfection. However, CD8+ T cells appear to be unnecessary against reinfection [46]. Development of a protective vaccine for prevention of *Chlamydia* PID is challenging due to difficulties in identifying and delivering relevant T cell antigens and developing a safe adjuvant that does not produce excessive inflammatory responses which can diminish the likelihood of public acceptance [47-49].

Studies need to be done to understand how to inhibit *C.t* infection becoming serious, and how to improve the prospects for development of a vaccine against *C.t* infection. These are the topics for the study of the dissertation.

2.2 Chlamydia pneumoniae

Chlamydia pneumoniae (*C.pn*) is an airborne chlamydial species responsible for human respiratory infection. It's also associated with atherosclerosis, coronary heart disease, and hyperlipidemia [50]. *C.pn* needs to persist within the infected tissues for periods of time to stimulate a chronic inflammatory response. The inflammation activated by *C.pn* is known to play an important role in the pathogenesis of atherosclerosis [51, 52]. *C.pn* has been shown to disseminate systemically from the lungs through infected peripheral blood mononuclear cells and to localize in arteries where it may infect endothelial cells, vascular smooth muscle cells, monocytes and macrophages and promote inflammatory atherogenous process [51, 53]. *C.pn* has recently been found in the human oral cavity and cause infectious diseases including caries, periodontitis, endodontitis, and tonsillitis [54]. We hypothesize that *C.pn* can infect oral epithelial cells and activate inflammation, which may further contribute to lung infections and heart diseases.

2.3 Chlamydia psittaci

Chlamydia psittaci (*C.pi*) usually infects birds but can be transmitted to humans by inhalation, contact or ingestion. The symptoms may differ due to the host. *C.pi* results in "fly-like" symptoms and even fatal cases of pneumonia [55, 56].

2.4 Chlamydia life cycle

Chlamydia is an obligate intracellular pathogen that can only survive and be transmitted with in host cells. All Chlamydia species share a common biphasic developmental cycle, during which they reside within a specialized vacuole, called an inclusion, within the host cell. During infection, chlamydia converts between two morphologically and functionally separate forms: the elementary body (EB) and the reticulate body (RB) [57, 58]. The EB is infectious but metabolically inactive, while RB is noninfectious and metabolically active. After internalization, the EB is surrounded by an endosome membrane and forms an inclusion. The inclusion allows a permissive environment to EB transform into a larger metabolically active RB, which replicates by dividing binary fission. After 40-48 hours, which may vary among different strains, the RBs transfer back into the EB and reseals from inclusion to cytosol and even neighboring cells [59, 60].

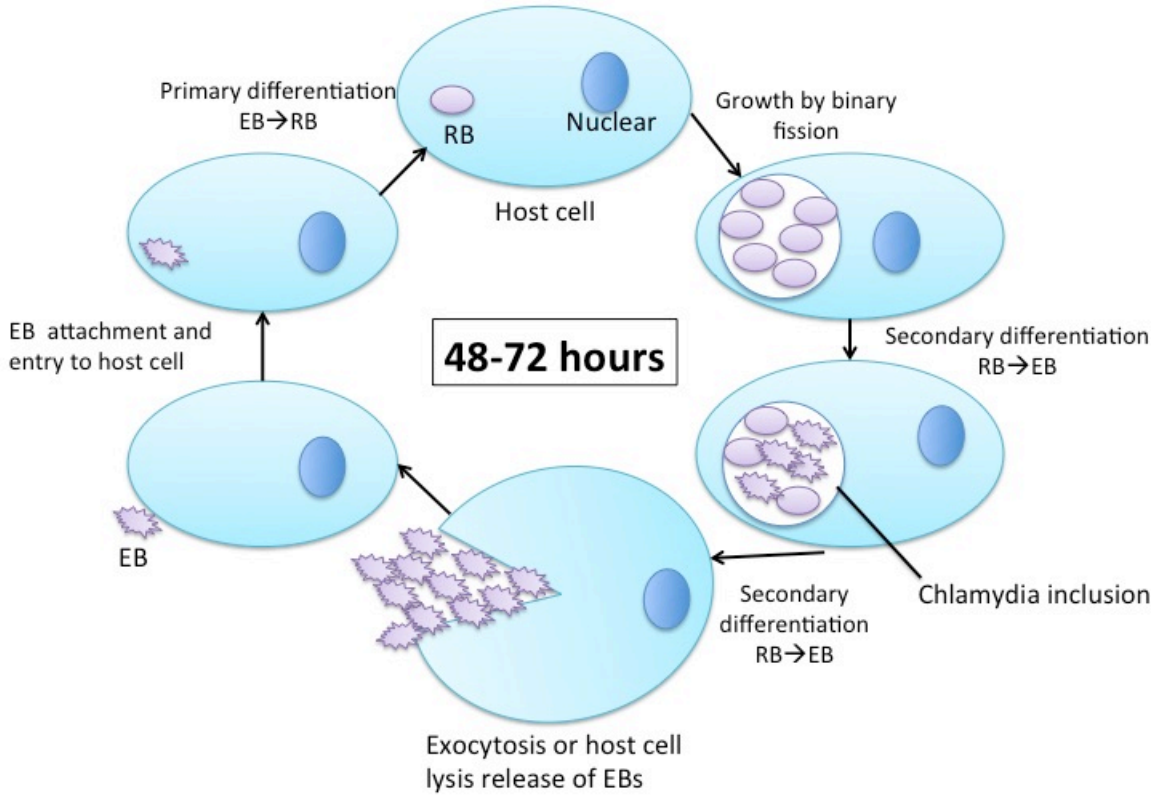

Figure 2. Life cycle of general Chlamydia species.

2.5 Immune response to Chlamydia infection

Chlamydia stimulates both the innate and adaptive immune response during infection. Lipopolysaccharide (LPS), the major surface antigen of Chlamydia, is recognized by PRRs including both TLRs and NLRs and up-regulates the expression of proinflammatory mediators. Studies have showed both TLR2 and TLR4 signaling via MyD88 are activated during infection and inducing early cytokine and chemokine production like IL-6 and IL-1b [61, 62]. These chemokine later recruits more immune cells like neutrophils, macrophages, dendritic cells and natural killer cells, resulting in more proinflammatory cytokines secreted to help with bacterial clearance [63]. However the release of cytokines may also cause chronic inflammation or tissue damage when the immune system fails to eliminate the bacteria. Therefore, it's important to study and develop methods to more successfully activate the innate immune response to clear bacteria and minimize the damage caused by chronic inflammation.

3. Vaults

Vaults were initially identified by Dr. Rome's lab in 1986 when preparing chlathrin-coated vesicles from rat liver, and were named due to their distinctive lobular morphology [64, 65]. Vaults are naturally occurring nanoparticles found widely in eukaryotes [66]. Vaults are classified as large cytoplasmic ribonucleoprotein particles (RNP) since they are composed of three protein species and a small-untranslated RNA. The most abundant protein in vaults is a 100 KD protein called major vault protein (MVP) that comprises over 70% of the particle mass. The other two proteins TEP1 and VPARP were also identified [67]. TEP1 is short for telomerase-associated protein 1, which is 290 KD. And VPARP, also known as PARP4, was determined to be related to the enzyme poly-(ADP-ribose) polymerase (PARP) [68, 69]. Moreover, the RNA component (vRNA) was shown to associate with TEP1 [69, 70].

Vaults have a cap-barrel-cap structure, which describes a protein shell containing multiple copies of MVP and a large central cavity. Vaults are highly conserved through evolution and ubiquitously distributed suggesting that vaults' function is essential and important, although its functionality remains mystery. Several findings show that vaults may potentially have a role in transport, drug resistance and innate immunity [71].

3.1 Engineering vaults

Vaults particles purified from rat liver are 13MDa and have a high conservation of copies of MVP. Studies showed that rat MVP sequence alone could directly express the formation of particles using the baculovirus system, so called engineering vaults [72]. The engineering vaults have similar morphology to endogenous vaults in that the center is empty (41nm×41nm×72.5nm) [73]. Its central hollow is large enough for copies of foreign material. Moreover, several studies indicate that vaults are non-immunogenic and highly stable in vitro, so it is ideal to engineer antigens into vaults' lumen and protect the immunogenic characteristics.

3.2 Vaults immunogenicity

As a naturally occurring nanoparticle, vaults appear to be an ideal structure to engineer for targeting tissues. It is reasonable to assume that vaults could be stable in the bloodstream since vaults are highly stable structures in vitro. Studies showed that vaults are non-immunogenic. Researchers have not found any antibodies that can be made to

purified-vaults [67]. In addition, in a nasal spray delivery model, the engineered vaults alone without any antigen inside failed to elicit an antibody response.

3.3 Smart adjuvant

An adjuvant is a pharmacological or immunological agent that is usually added to vaccines to enhance the recipient's immune response. The engineered vaults with antigen packaged inside behaved like "smart adjuvants", which could induce dendritic cells (DC) maturation and the secretion of cytokines and chemokine necessary for immune response, but did not cause DCs to secrete factors associated with tissue inflammation [74].

3.4 Chlamydia-vaults

As mentioned previously, most *Chlamydia* infections are asymptomatic, increasing the risk of transmission of *Chlamydia* to unsuspecting females and result in PID [42, 75, 76]. Identification of protective responses is a key component of vaccine development. Intensive studies have been done in order to dissect immunity towards to resolution of primary chlamydial infection, and immunity to reinfection in mouse genital infection model.

The full potential of vaccines relies on development of effective delivery systems and adjuvants and is critical for development of successful vaccine candidates. We have shown that vaults can be engineered *in vitro* as an engineered vaccine, which effectively delivers antigen to general a protective immune response. However, we and other groups have also discovered that recombinant vaults could interact with host immune cells and display self-adjuvanting properties, distinguishing them from other vaccine preparations [71, 77-79]. Moreover, we reported that vaults engineered to contain a recombinant *Chlamydia* protein (MOMP-vault vaccine) induced strong protective anti-chlamydial immune responses without eliciting excessive inflammation as measured by TNF-α production [74]. We will refer to this recombinant vault with MOMP as Chlamydial-vaults hereafter. We hypothesized that Chlamydial-vaults act as "smart adjuvants" and can be engineered to produce a tailored immune response against specific antigens by housing proteins in the central cavity of the recombinant vault that is hollow and large enough to accommodate multiple copies of foreign epitopes [74, 77]. Our data further suggests that the Chlamydial-vaults induced inflammasomes, an innate immune

response that could possibly account for the self-adjuvanting property of vault-vaccines upon phagocytosis.

Chapter 2 Materials and Method

2.1 Cell culture, bacteria and treatment

2.1.1 THP-1 cells with Chlamydia-vaults

Human acute monocyte leukemia cell lines (THP-1) were obtained from American type Culture Collection (ATCC). THP-1 cells were grown in RPMI 1640 (Sigma-Aldrich) with 10% FBS (Invitrogen) and 10μg/ml gentamicin. Chlamydia-vaults were obtained from UCLA (Dr. Kathleen's lab) and kept in 4°C before treatment.

A total of 1×10^6 cells per well in a 6-well plate were differentiated with 500 nM Phorbol 12-myristate 13-acetate (PMA) for 3 hours. Differentiated THP-1 cells were washed with 1XPBS three times and incubated for 24 hours at 37°C with 5% CO_2. Caspase-1 inhibitor Z-WEHD (100 nM) and Cathepsin B inhibitor CA-074 Me (10 μM) were applied to treat cells 1.5 hours before chlamydia-vaults infection. Syk-inhibitor (10 μM) was used 30 minutes prior to addition of chlamydia-vaults. Chlamydia-vaults (250 nM) were incubated with cells, and after 6 hours post-incubation, we collected the supernatant from the treated cells.

2.1.2 GEC cells with C.pn

Gingival epithelial cells (GECs) were obtained from Dr. Ozlem's lab (Gainesville, FL). GEC cells were grown in defined keratinocyte-SFM (1X) media (KM) (Invitrogen) containing 10% heat-inactivated fetal bovine serum (FBS), L-glutamine, bovine pituitary extract (BPE), and embryonic growth factor (EGF). GEC cells were grown in a humidified incubator at 37 °C with 5% CO_2.

Chlamydia pneumoniae (C.pn) was obtained from Dr. Arditi's lab (UCLA). GEC cells growing at 60% confluency on 6-well plates were infected with the C.pn at multiple multiplicities of infection (MOI.), and incubated usually 72hours in an incubator at 37 °C with 5% CO_2.

2.2 Gene product depletion by RNA interference

THP-1 cells stably expressing shRNA against NRLP3, ASC, Syk and caspase-1 were obtained by transducing THP-1 cells with lentiviral particles containing shRNA. (Sequences are listed in Table 2.1) The shRNA was used separately to silence gene expression following the manufacturer's instructions. Non-target shRNA control cells were also generated using an irrelevant sequence (Sigma; catalog number SHC002 V).

Cells (3×10^5) were plated at 35% confluency 24 hours prior to transduction and then the corresponding lentiviral transduction particles were added at an MOI of 3 overnight. Fresh media were added the next day, and transduced cells were selected by addition of media containing 2μg/ml puromycin (Sigma). The knockdown (KD) efficiency was tested by real-time PCR. mRNA was isolated from cells after indicated treatments or incubations using the Qiagen RNeasy Kit (Qiagen, Valencia, VA) following the manufacturer's instruction.

Table 2.1: Sequences of shRNA used to silence gene expression.

	Sequence	Cat. No
NLRP3	5'-CCGGGCGTTAGAAACACTTCAAGAACTCGAGTTCTTGAAGTGTTTCT AACGCTTTTTG-3'	NM_004895
ASC	5'-CCGGCGGAAGCTCTTCAGTTTCACACTCGAGTGTGAAACTGAAGAG CTTCCGTTTTTG-3'	NM_013258
Syk	5'-CCGGGCAGGCCATCATCAGTCAGAACTCGAGTTCTGACTGATGATG GCCTGCTTTTT-3'	NM_003177
Caspase -1	5'-CCGGGAAGAGTTTGAGGATGATGCTCTCGAGAGCATCATCCTCAAA CTCTTCTTTTT-3'	NM_001223
	5'-CCGGTGTATGAATGTCTGCTGGGCACTCGAGTGCCCAGCAGACATT CATACATTTTT-3'	
	5'-CCGGCTACAACTCAATGCAATCTTTCTCGAGAAAGATTGCATTGAG TTGTAGTTTTT-3'	
	5'-CCGGCCAGATATACTACAACTCAATCTCGAGATTGAGTTGTAGTAT ATCTGGTTTTT-3'	

2.3 IL-1β & TNF-α ELISA assay

Supernatants from treated cells were collected after post-incubation and stored at −80°C until ready for use in the assay. Measurement of IL-1β was carried out using human IL-1β ELISA kit (eBioscience, San Diego, CA), following manufacturer's instructions.

2.4 Western blotting

Supernatants from treated cells were collected and precipitated with TCA protein precipitation protocol. Briefly, 100% (w/v) Trichloroacetic acid (TCA) recipe was prepared. One volume of TCA stock to four volumes of protein sample was added and incubated 10 minutes at 4°C. Centrifuge the samples at 14K Revolution(s) Per Minute (rpm) for 5 minutes. Pellets were washed with acetone and heated in 95°C for 5 to 10 minutes.

Samples were lysed using 1× RIPA Lysis Buffer (Millipore) with 1× protease inhibitor cocktail (Biovision) and loaded onto a 12% SDS-polyacrylamide gel and then transferred to a polyvinylidene difluoride membrane (Millipore). For detection of the active caspase-1 subunit, the blot was probed with 1 mg/ml rabbit anti-human caspase-1 antibody (Millipore), and then incubated again with conjugated 1:10000 dilution of anti-rabbit IgG horseradish peroxidase (Millipore). To detect mature IL-1β, the blot was probed with IL-1β antibody (Cell Signaling) at a 1:1000 dilution, and then incubated again with 1:10000 dilution of anti-mouse secondary antibody (Santa Cruz Biotechnology). Western blotting detection reagents (Amersham Biosciences) were used following manufacturer's instructions and chemiluminescence was detected using a gel doc system (Bio-Rad).

2.5 Fluorescence-activated cell sorting (FACS)

THP-1 cells (2×10^6/well) were plated in 6-well plates and primed for 3 hours with 0.5 μM PMA (Sigma-Aldrich, St. Louis, MO). Chlamydia-vaults were dual-labeled with the fluorescent dyes FITC and TRITC by primary amine reaction following manufacturer's instructions (Pierce, Thermo Scientific, Rockford, IL). Unconjugated dye was removed by filtration on a PD-10 column (GE Healthcare, Piscataway, NJ). Primed THP-1 cells were incubated in duplicate with FITC-TRITC dual-labeled vaults for 6, 18, 24 or 48 hours. Half of the treatments were incubated with bafilomycin (Sigma-Aldrich, St. Louis, MO), an ATPase inhibitor, for 30 minutes to neutralize all subcellular compartments. Cells were collected by trypsinization, washed and immediately analyzed by flow cytometry using a BD FACSCalibur (BD Biosciences, Franklin Lakes, New Jersey) and

data was analyzed using Flowjo software (Tree Star, Inc., Ashland, OR). A total of 10^5 cells were analyzed.

For FACS analysis of lymphocytes, the spleen was harvested from individual mice, and single cell suspensions were prepared by dissociating the lymphocytes through a 40-μm-cell strainer (BD Falcon). Individual cells were washed with 1% PBS followed by red blood cell lysis treatment. Lymphocytes were re-suspended in RPMI 1640 at 4°C until used. For intracellular cytokine staining, lymphocytes isolated from spleen were incubated in RPMI 1640 in the presence of PmpG-1303–311 peptide for 6–8 hours. Brefeldin A (Sigma) was added 4 hours before the end of culture. Cells were directly stained with fluorochrome-labeled antibodies against CD3 (clone 145–2C11) or CD4 (clone GK1.5). After washing, the cells were incubated with Cytofix/Cytoperm (BD Biosciences) for 1 h and stained with fluorochrome-conjugated anti-IFN-γ (clone XMG1.2), washed again, re-suspended in Cell Fix solution, and analyzed on a SORP BD LSR II (Beckman Dickinson, Franklin Lakes, NJ). FACS data were analyzed by Flowjo (Tree Star, Oregon).

2.6 Chlamydia, immunization and challenge of mice

Chlamydia muridarum (*MoPn*) was grown on confluent McCoy cell monolayers, purified on Renograffin gradients and stored at −80°C in SPG buffer (sucrose-phosphate-glutamine) as previously described [48]. Female C57BL/6 mice, 5–6 weeks old were housed according to American Association of Accreditation of Laboratory Animal Care guidelines [48]. Mice receiving vaults were anesthetized with a mixture of 10% ketamine plus 10% xylazine and immunized i.n. with 100 μg chlamydia-vaults in 20 μl saline for a total of 3 times every two weeks. Mice were hormonally synchronized by subcutaneous injection with 2.5 mg of medroxyprogesterone acetate (Depo Provera, Upjohn, Kalamazoo, MI) in 100 μl saline 7 days prior to a vaginal challenge with 1.5×105 IFU of C. muridarum and infection was monitored by measuring infection forming units (IFU) from cervical-vaginal swabs (Dacroswab Type 1, Spectrum Labs, Rancho Dominguez, CA) as previously described [48].

2.7 Colocalization studies

The following antibodies were used for immunofluorescence at the indicated dilutions: anti-early endosome antigen 1 (EEA1, G-4; 1:100; Santa Cruz Biotechnology, Dallas, TX), anti-lysosomal-associated membrane protein1 (LAMP1, clone H4A3; 1:100; Biolegend, San Diego, CA), anti-microtubule-associated protein 1 light chain 3 (LC3, clone 166AT1234; 1:100; Abgent, San Diego, CA), and AF488-goat anti-mouse

immunoglobulin G (IgG; 1:400; Invitrogen, Carlsbad, CA). For colocalization studies, THP-1 cells (1.5 × 105) were seeded onto 18 mm glass coverslips and incubated at 37 °C (with 5% CO2) for 72 hours in the presence of 10 ng/ml PMA. Purified PmpG-1-vaults vaults were labeled with DyLight 650 according to the manufacturer's instructions (Pierce, Thermo Scientific, Rockford, IL). Coverslips containing primed THP-1 cells were incubated with 30 μg of DyLight 650-labeled chlamydia-vaults for 15 min, 30 min, and 1 h. Cells were fixed in 3.7% paraformaldehyde in 1× PHEM buffer (60 mM Pipes, 25 mM Hepes, 10 mM EGTA, 2 mM MgCl2) for 15 minutes at room temperature. Cells were washed 3 times in 1× PHEM buffer before permeabilization for 10 minutes in 0.25% Triton X-100 in 1× PHEM buffer. Following permeabilization, the cells were washed 3 times in 1× PHEM buffer prior to incubation in blocking solution (10% normal goat serum in 1× PHEM buffer) for 1 h at room temperature. Cells were further incubated with the appropriate primary antibody diluted in blocking solution for 1 h at room temperature, rinsed 3 times in 1× PHEM buffer and further incubated for 1 h in secondary antibody prepared in blocking solution. Following staining with the secondary antibody, the cells were washed 3 times with 1× PHEM buffer and mounted in VectaShield Hard Mount with DAPI (Vector Labs, Inc., Burlingame, CA) and visualized using a Yokagawa CSU-22 spinning disc confocal scanner and a Hamamatsu C9100–13 EMCCD camera mounted on a Zeiss Axiovert 200m stand. The images were captured using Slidebook 5 software (Intelligent Imaging Innovations, Inc., Denver, CO). The optimal conditions including the number of vault particles used for each experiment were determined empirically. Images were acquired with a 100× oil immersion objective and were processed using ImageJ (http://rsb.info.nih.gov/ij/). In addition, 10 images were used to determine colocalization by applying the Pearson's correlation coefficient located in the JACoP Plugin module.

2.8 RNA isolation, PCR and Real Time PCR

RNA was isolated from cells after treatments using Trizol Reagent (Invitorgen) following the manufacturer's instructions. In brief, 1 ml Trizol per well was added into 6-well plates. Incubating for 5 minutes, cells were collected and 200ul chloroform (Sigma-aldrich) was added with 15 seconds shaking. Samples were spun down at 12,000g for 15 minutes and transferred into a new 1.5ml tube. 500ul isopropanol (Sigma-aldrich) was added and incubated for 10 min before next 10min centrifuge. Pellet was washed with 100% ethanol (Sigma-Aldrich) and then left for air-dry. Mixed with RNase-free water with appropriate amount and heated in 60°C for 10 min.

RNA concentration was measured using a Nanodrop (Thermo Scientific, Wilmington, DE), and total RNA was converted into cDNA by standard reverse transcription with

Taqman reverse transcriptase kit (Applied Biosystems, Foster City, CA). Quantitative PCR was performed with 1:50 of the cDNA preparation in the Mx3000P (Stratagene, La Jolla, CA) in a 25 µl final volume with Brilliant QPCR master mix (Stratagene). The primers sequences used are summarized in Table 2.2.

Table 2.2: Sequences of primers used to proceed.

Gene	Sequence
GAPDH forward	5'-CTTCTCTGATGAGGCCCAAG-3'
GAPDH reverse	5'-GCAGCAAACTGGAAAGGAAG-3'
NLRP3 forward	5'-CTTCCTTTCCAGTTTGCTGC-3'
NLRP3 reverse	5'-TCTCGCAGTCCACTTCCTTT-3'
ASC forward	5'-AGTTTCACACCAGCCTGGAA-3'
ASC reverse	5'-TTTTCAAGCTGGCTTTTCGT-3'
SYK forward	5' AGAGCGAGGAGGAGCGGGTG-3'
SYK reverse	5'-CCGCTGACCAAGTCGCAGGA-3'
IL-1b forward	5'-CAGCCAA TCTTCA TTGCTCA-3'
IL-1b reverse	5'-TCGGAGATTCGTAGCTGGAT-3'
IL-8 forward	5'-AATCTGGCAACCCTAGTCTGCTA-3'
IL-8 reverse	5'-AGAAACCAAGGCACAGTGGAA -3'
C.pn forward	5'-TTATTAATTGATGGTACAATA -3'
C.pn reverse	5'-ATCTACGGCAGTAGTATAGTT-3'

2.9 Immunocytochemical staining and fluorescence microscopy

GEC cells were grown on coverslips (Fisher brand) and then infected with *C.pn* and incubated at 37 °C. After treatment for 72 hours, supernatant was aspirated. Cells on the coverslips were fixed with freezing cold methanol for 10 minutes and washed with 1XPBS three times. 0.1% of Tritonx100/ PBS was used to permeabilize cells for 15 minutes and 5% BSA/PBS was used to block the cells for an hour. Cells were then stained with IMAGEN Chlamydia (Imagen) in humid environment for 15 minutes. During the last 5 min of incubation, Hoechst 3342 stain (Sigma) was added, and then cells were washed three times with PBS for 5 minutes each time. Coverslips were mounted with cells side down on glass slides using a small drop of mounting medium and then sealed to the slides with nail polish, and finally viewed on a wide field fluorescence microscope (Leica, Deerfield, IL).

2.10 Clinical samples preparation and PCR

Dental plaque from subgingival periodontal pockets was collected using sterile Gracey curettes. Plaque from the curette was transferred into 350 ul of RTF buffer (0.045% K_2HPO_4, 0.045% KH_2PO_4, 0.09% NaCl, 0.09% $(NH4)_2SO_4$, 0.018% $MgSO_4$, 0.038% EDTA, 0.04% Na_2CO_3, 0.02% dithiothreitol) [80]. Plaque samples were collected from 10 patients. Two healthy sites and two periodontics sites were collected from each patient. The sites are shown in the following table 2.3.

Table 2.3: Positions of sites of Clinique samples.

Patient No.	Healthy site A	Healthy site B	Diseased site C	Diseased site D
1	6DB	7DB	5DB	29DB
2	7B	10B	2MB	3DL
3	8DB	9MB	14DL	31ML
4	7MB	6MB	29DL	31ML
5	5B	6B	2DL	12DB
6	11B	10B	19DL	18ML
7	27B	6B	31DL	32ML
8	8B	6B	21DL	2DL
9	8MB	7B	6MB	2DB
10	10B	11B	3MB	2DB

All the samples were incubated in 95°C for 10 minutes, and PCR was performed to amplify bacteria DNA using Taqman PCR kit. (Qiagen). A hot-start protocol was used in which samples were preheated at 94°C for 4 min, followed by amplification using the following conditions: denaturation at 94°C for 45 s, annealing at 60°C for 45 s, and elongation at 72°C for 2 min, with an additional 1 s for each cycle. Thirty five cycles were performed, followed by a final elongation step at 72°C for 15 min. Amplicon size and amount were examined by electrophoresis in a 2% agarose gel stained with a final concentration of approximately 0.5μg/mL ethidium bromide (EtBr) (Invitrogen, Carlsbad, CA) and visualized under UV light. Purified *C.pn* strain was applied as a positive control.

Chapter 3. Results: Activation of the NLRP3 inflammasome by vault nanoparticles expressing a chlamydial epitope.

3.1 Chlamydia-vaults activate the NLRP3 inflammasome and induce IL-1β secretion, as measured by an ELISA assay.

THP-1 is a human monocytic cell line that can be differentiated into macrophage-like cells upon priming with phorbol-12-myristate-13-acetate (PMA). It synthesizes pro-IL-1β thereby serving as a good model for studying inflammasome activation. To evaluate whether chlamydia-vaults induce inflammasome activation, we measured IL-1β secretion from PMA-primed THP-1 cells incubated with chlamydia-vaults containing the chlamydial epitope, PmpG. After 6 hours of incubation, significantly higher levels of IL-1β were detected in the supernatants from chlamydia-vaults treated than untreated cells (Figure 3A).

Empty vaults without any epitope were also tested and no induction of immune response could be detected (data not shown) [74]. Therefore they were not included in the experimental setting hereafter. To determine whether IL-1β secretion induced by chlamydia-vaults is dependent on caspase-1 activation, we incubated the cells with a caspase-1 inhibitor, z-WEHD-fmk [81]. This inhibitor also blocks caspase-4 and caspase-5, which could potentially modulate inflammasome activity [37]. Upon pre-treatment of cells with z-WEHD-fmk, chlamydia-vaults induced dramatically decreased levels of IL-1β secretion (Figure 3A). Meanwhile, the levels of activated caspase-1 were also examined by ELISA and Western blot analyses. While chlamydia-vaults stimulated a dramatic secretion of mature caspase-1, z-WEHD-fmk treatment efficiently blocked caspase-1 activation as expected (Figure 3C).

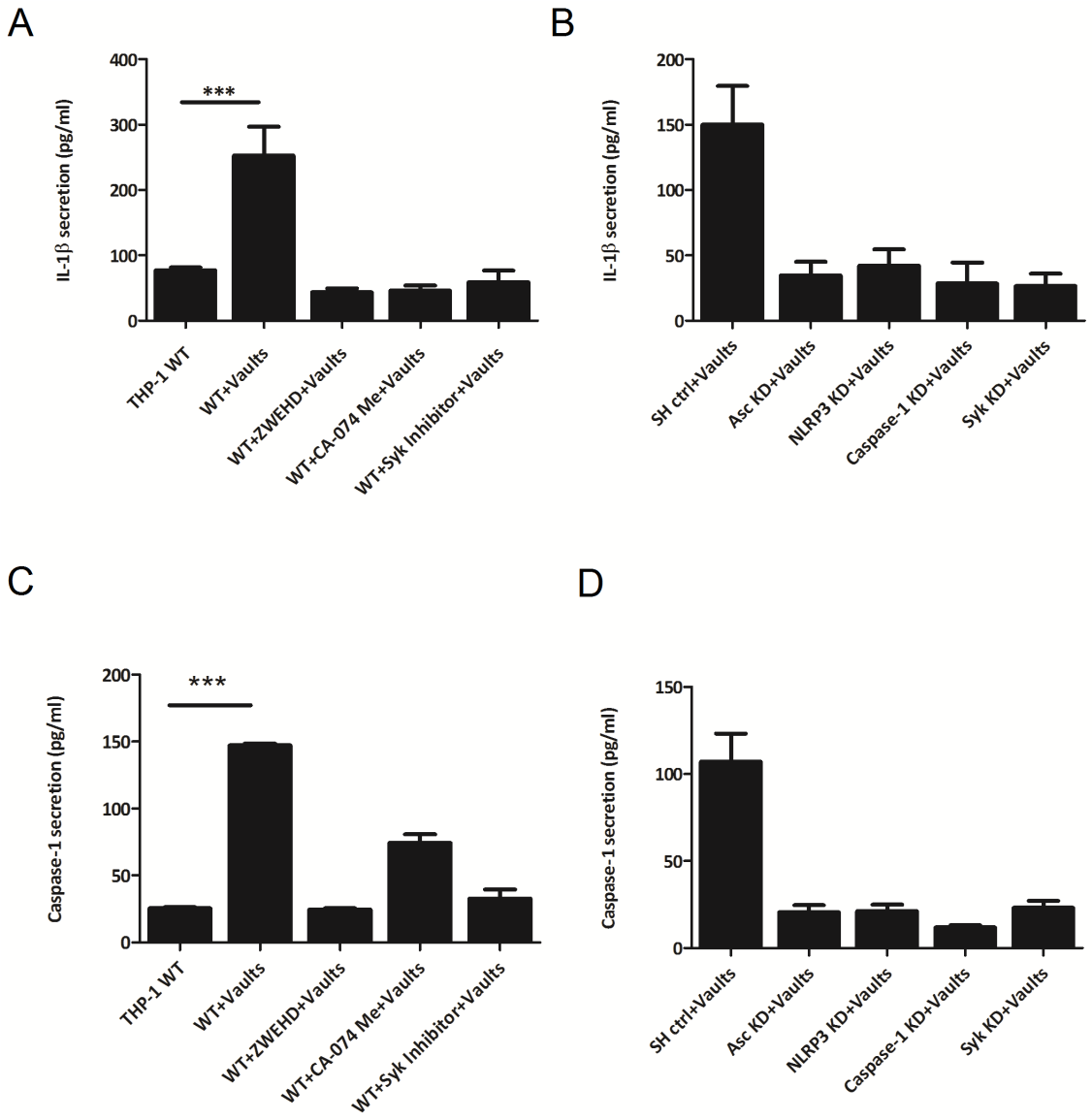

Figure 3 PmpG-1-vaults activate the NLRP3 inflammasome and induce IL-1 secretion, as measured by an ELISA assay. THP-1 (1×10^6) wild type (WT) cells (A) were incubated in 6-well plates with RPMI 1640 media. Inhibitors of caspase-1 (ZWEHD) or cathepsin B (CA-074) were added individually 1.5 hour prior to incubation with PmpG-1-vaults, and the Syk inhibitor was added 0.5 h prior to incubation with PmpG-1-vaults. THP-1 knockdown (KD) cells (B) were incubated with media alone, and 500 g of PmpG-1-vaults were added to each well, except the WT control ($p < 0.001$). (C) THP-1 (1×10^6) WT cells were incubated in 6-well plates. ZWEHD or CA-074 was added individually 1.5 h prior to incubation with PmpG-1-vaults, and the Syk inhibitor was added 0.5 hour prior to incubation with PmpG-1-vaults. (D) THP-1 knockdown (KD) cells were incubated with media alone, and 500 g of PmpG-1-vaults were added to each well, except the WT control. The mean ± SD of a representative experiment from six times was analyzed by ANOVA. In all cases, cell supernatants were measured in triplicate.

3.2 Incubation of cells with PmpG-1-vaults activates the NLRP3 Inflammasome

The NLRP3 inflammasome could be activated by a broad range of stimuli, such as nanoparticles and crystals [82]. We have demonstrated that chlamydia-vaults is able to induce IL-1β and caspase 1 secretion from THP-1 cells. To further investigate the mechanism by which PmpG-1-vaults activate the NLRP3 inflammasome, we focused on several representative NLRP3 components that are involved in inflammasome pathway. These include the NLR family member NLRP3, the adaptor protein ASC, the protease caspase-1, and the mediators Syk and cathepsin B. To test whether these components play a role in vault-induced IL-1β secretion, we either applied inhibitors against each component or depleted some components by RNA interference. When CA-074 Me, an inhibitor of cathepsin B, was incubated with cells 1.5 hours before incubation with PmpG-1-vaults, there was a large inhibition of IL-1β secretion (Figure 3A). In contrast, the inhibitor alone had no effect on IL-1β secretion (data not shown). Similarly, pre-incubation with a Syk inhibitor for 30 minutes significantly decreased chlamydia-vaults induced IL-1β secretion (Figure 3A). These results suggest that both Syk recruitment and lysosomal destabilization are involved in vault-induced inflammasome activation. To specifically probe for NLRP3 inflammasome activation by the chlamydia-vaults, we depleted ASC and NLRP3 using shRNA approach delivered by lentiviral particles. THP-1 cells were either treated with a non-silencing shRNA control, or lentiviral constructs selectively knock down ASC, Syk, caspase-1, and NLRP3

As compared to the non-silencing control, THP-1 cells depleted for either gene expression produced dramatically decreased levels of IL-1β upon stimulation with chlamydia-vaults (Figure 3B). These results reinforce our conclusion that PmpG-1-vaults induce IL-1β secretion via NLRP3 inflammasome activation. Next, we measured caspase-1 activation in the presence of inhibitors against upstream mediators of the NLRP3 inflammasome. The cathepsin B inhibitor, CA-074 Me, dampened chlamydia-vaults mediated caspase-1 activation by approximately half, suggesting that lysosomal disruption may be involved in this process. In addition, the Syk inhibitor also strongly decreased caspase-1 activation (Figure 3C). To further confirm the specificity of these inhibitors on NLRP3 inflammasome inhibition, we verified the effect of inflammasome gene silencing on caspase-1 activation. As expected, depletion of the respective target genes (NLRP3, ASC, and Syk) by RNA interference significantly dampened PmpG-1-vault-induced caspase-1 activation in THP-1 cells (Figure 3D). Moreover, there was also less caspase-1 activation when the cells were depleted of caspase-1 (Figure 3D). The knockdown efficiency of the respective shRNA constructs was confirmed by qPCR (Figure 6). In addition to the results on processed IL-1β and activated caspase-1 secretion obtained by ELISA (Figure 3), we also confirmed the protein levels of mature IL-1β and activated caspase-1 in the cell culture supernatant by Western blot (Figure 4). Incubation of THP-1 cells with PmpG-1-vaults stimulated secretion of mature IL-1β in the supernatant, which could be inhibited by pre-incubation with the caspase-1 inhibitor z-WEHD-fmk (Figure 4A and B). Similarly, activated caspase-1 could be detected in the

supernatant of PmpG-1-vault-stimulated THP-1 cells, and its levels could be inhibited by z-WEHD-fmk (Figure 4C and D). To further confirm the functional specificity of the shRNA depletion of the inflammasome gene expression, the respective THP-1 cell lines were primed with 10 μg/ml LPS and the TNF-α secretion was measured by ELISA, as secretion of this cytokine takes place through an inflammasome-independent pathway. As expected, depletion of inflammasome-associated components had no effect on LPS-induced TNF-α production in THP-1 cells (Figure 5), demonstrating that shRNA-mediated depletion of caspase-1, ASC, NLRP3 and Syk specifically affected cytokine secretion via inflammasome-dependent pathway. Taken together, these results demonstrate that the chlamydia-vaults vaccines can activate caspase-1 and stimulate IL-1β secretion through a signaling cascade involving the NLRP3 inflammasome.

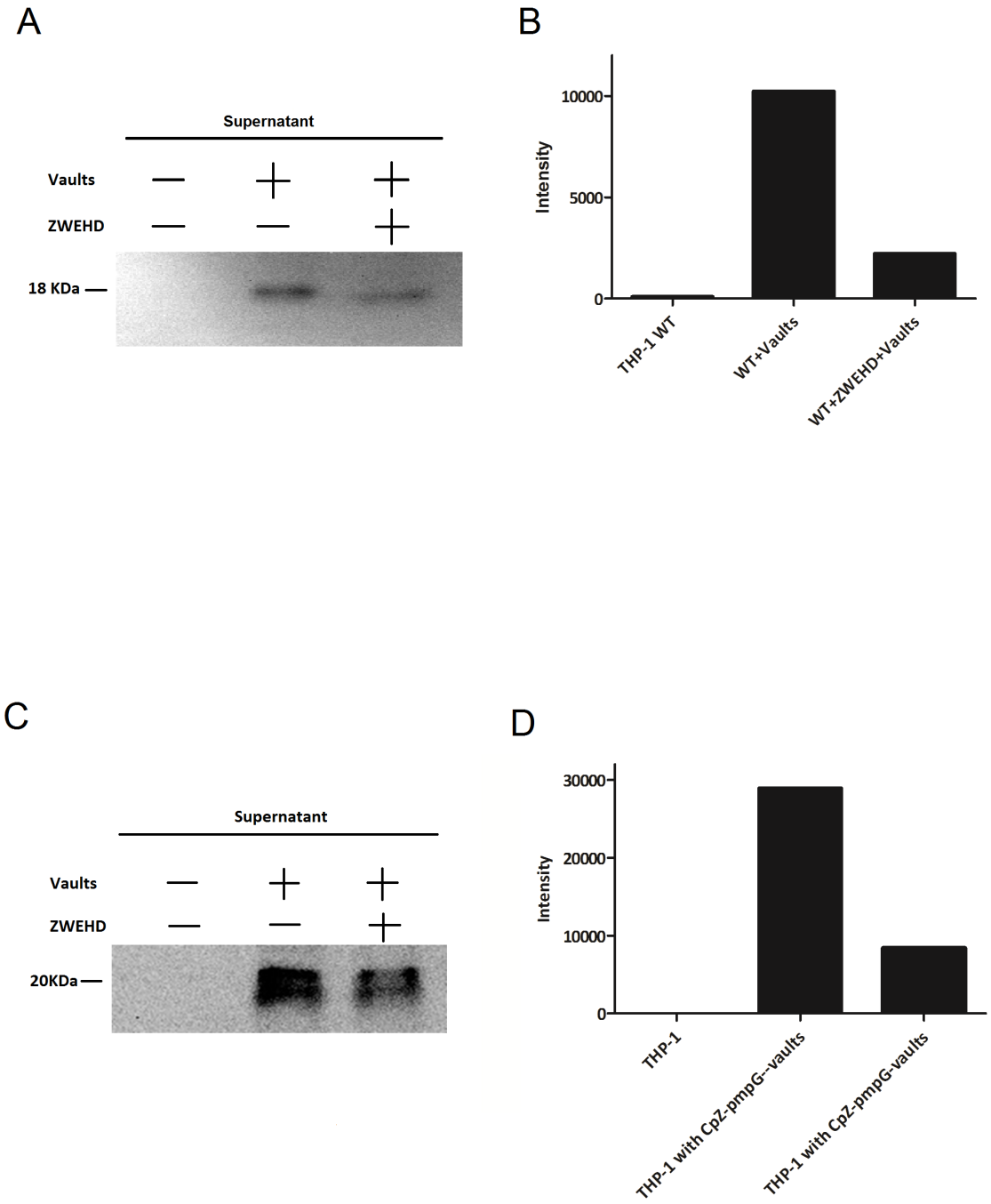

Figure 4 Activation of NLRP3 inflammasome by Chlamydia-vaults leads to caspase-1 and IL-1β maturation. THP-1 (1×10^6) wild type (WT) cells (A) were incubated in 6-well plates with RPMI 1640 media. ZWEHD was added 1.5 h prior to incubation with PmpG-1-vaults. THP-1 knockdown (KD) cells (B) were incubated with media alone, and 500 g of PmpG-1-vaults were added to each well, except the WT control. Culture supernatants were collected 6 hours post-incubation and IL-1 or caspase-1 were detected by Western blot. (A) Western blot of the supernatant probed for IL-1. (B) Histogram showing the intensity of the bands in the Western blots. (C) Western blots of the supernatant probed caspase-1. (D) Histogram showing the intensity of the bands in the Western blots.

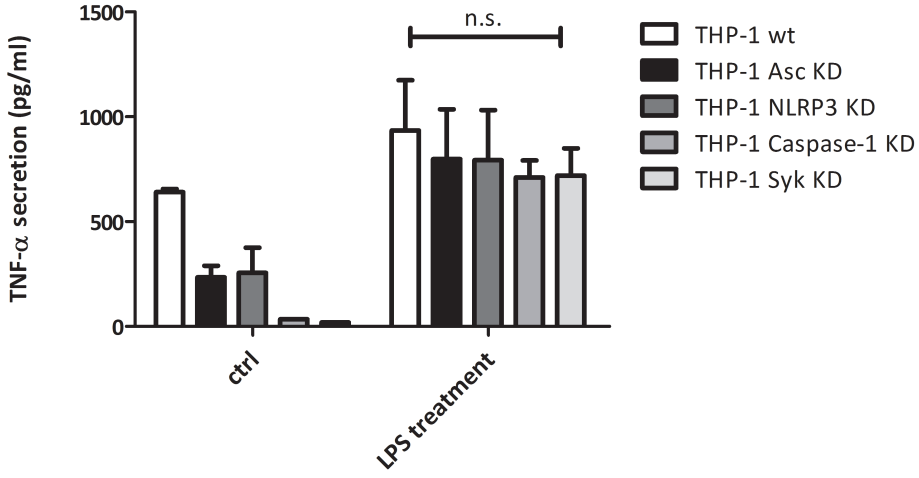

Figure 5 Depletion of inflammasome-related genes does not affect TNF-a levels. THP-1 (1×10^6) knockdown (KD) cells were incubated in 6-well plates with RPMI 1640 media. LPS (100 ng/ml) was added as stimulator. Culture supernatants were collected 24 hours post-incubation, and TNF-a was measured by ELISA. TNF-a levels from WT cells were compared to KD cells stimulated by LPS. The values for the WT and KD cells were not statistically significant: $p < 0.5$ for WT vs caspasd-1 KD, and $p < 0.5$ for WT vs Syk KD cells.

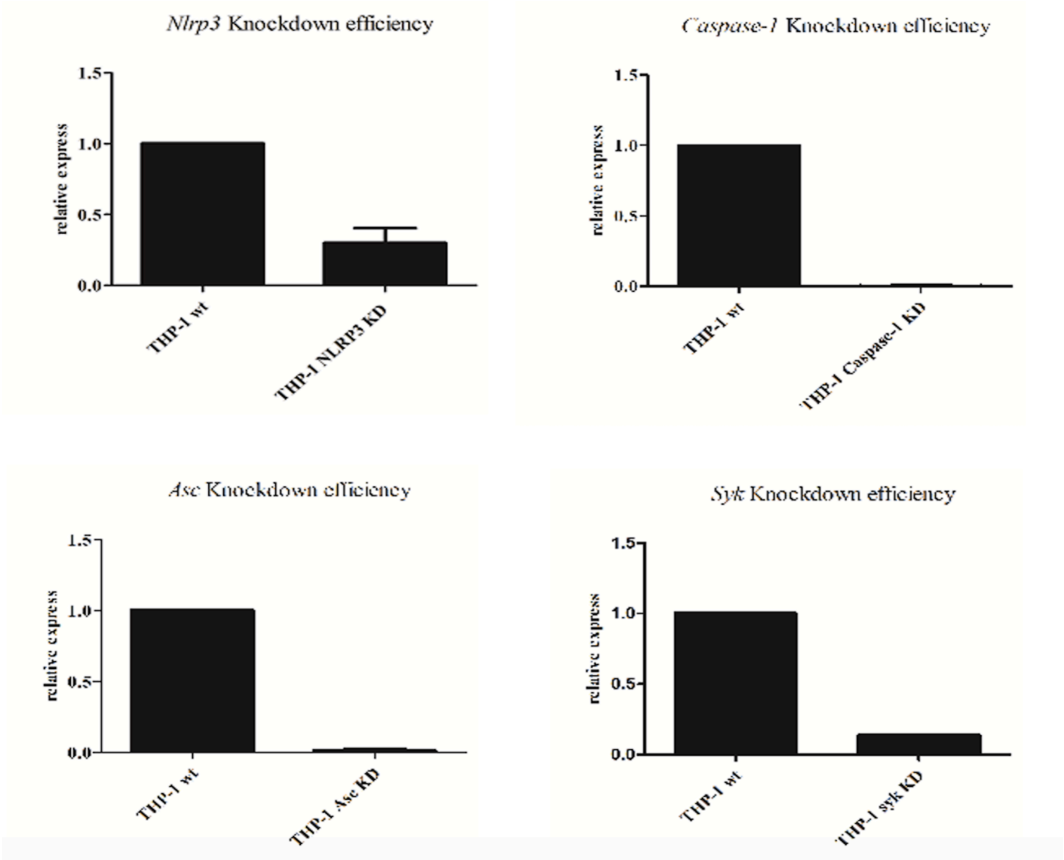

Figure 6 The knockdown efficiency of NLRP3, ASC, Caspase-1, and Syk in THP-1 cells. Efficiency was measured by real-time PCR. Ct values are normalized to GAPDH and relative expression (ΔΔCt) is calculated compared to non-infected cells.

3.3 Internalized Chlamydia-vaults co-localize with lysosomes

We next investigated the intracellular trafficking of chlamydia-vaults after their uptake by THP-1 cells. Chlamydia-vaults were dually labeled with FITC (green) and TRITC (red) (Figure 7A) and examined for intracellular localization by flow cytometry (Figure 7B). As the fluorescence of FITC is sensitive to pH, this labeling strategy allows us to determine whether the particles enter an acidic compartment after internalization. In parallel, one group of cells was treated with bafilomycin to prevent re-acidification of vesicles before incubation with chlamydia-vaults. While the majority of chlamydia-vaults were in acidic compartments after 6 hours of incubation, most of them were at neutral pH after 24 hours (Figure 7C). These results indicate that following phagocytosis, the majority of PmpG-1-vaults are internalized initially into acidic compartments (endolysosomes or phagolysosomes), from which they escape into the cytosol.

To further address the intracellular localization of chlamydia-vaults, we examined their co-localization with cellular compartment markers by confocal fluorescence microscopy. The chlamydia-vaults were labeled with DyLight650 and EEA1, Lamp1, and LC3 were selected for markers of early endosome, lysosome, and auto-phagosome, respectively (Figure 8). After 15 min, 30 min and 60 min, approximately 40% of chlamydia-vaults co-localized extensively with EEA1 and Lamp1 (Figure 8), as calculated by a significant Pearson's coefficient. This indicates that the majority of chlamydia-vaults were internalized into lysosomes, which led to lysosomal disruption. These results are in agreement with previous observation that inhibitors of cathepsin B block NLRP3 inflammasome activation in cells incubated with chlamydia-vaults.

3.4 Immunization with chlamydia-vaults induces an immune response in vivo

Given that chlamydia-vaults elicit strong activation of NLRP3 inflammasome *in vitro*, we next examined its immunogenicity *in vivo*. To this end, mice were vaccinated vaginally with the chlamydia-vaults vaccine, and the immune responses were monitored. Spleen cells were harvested from naïve mice as well as from mice that were immunized with chlamydia-vaults three times. Two weeks after the last immunization, all mice were sacrificed and the lymphocytes were isolated from spleens and stimulated *in vitro* overnight. Single cell suspensions were analyzed by flow cytometry for expression of CD3, CD4, and IFN-γ, which are markers for Th1 helper cells, and were gated on cells that are specific for MHC peptide tetramers containing a peptide derived from PmpG-1 (Figure 9). We observed that the cells from immunized mice contained a larger

percentage of specific Th1 cells within the $CD4^+$ cell population than cells from naïve mice did. Taken together, these results demonstrate that the foreign epitope incorporated into the PmpG-1-vault vaccine is accessible to the immune system *in vivo*, which could be harnessed to elicit effective immune response to chlamydia antigens.

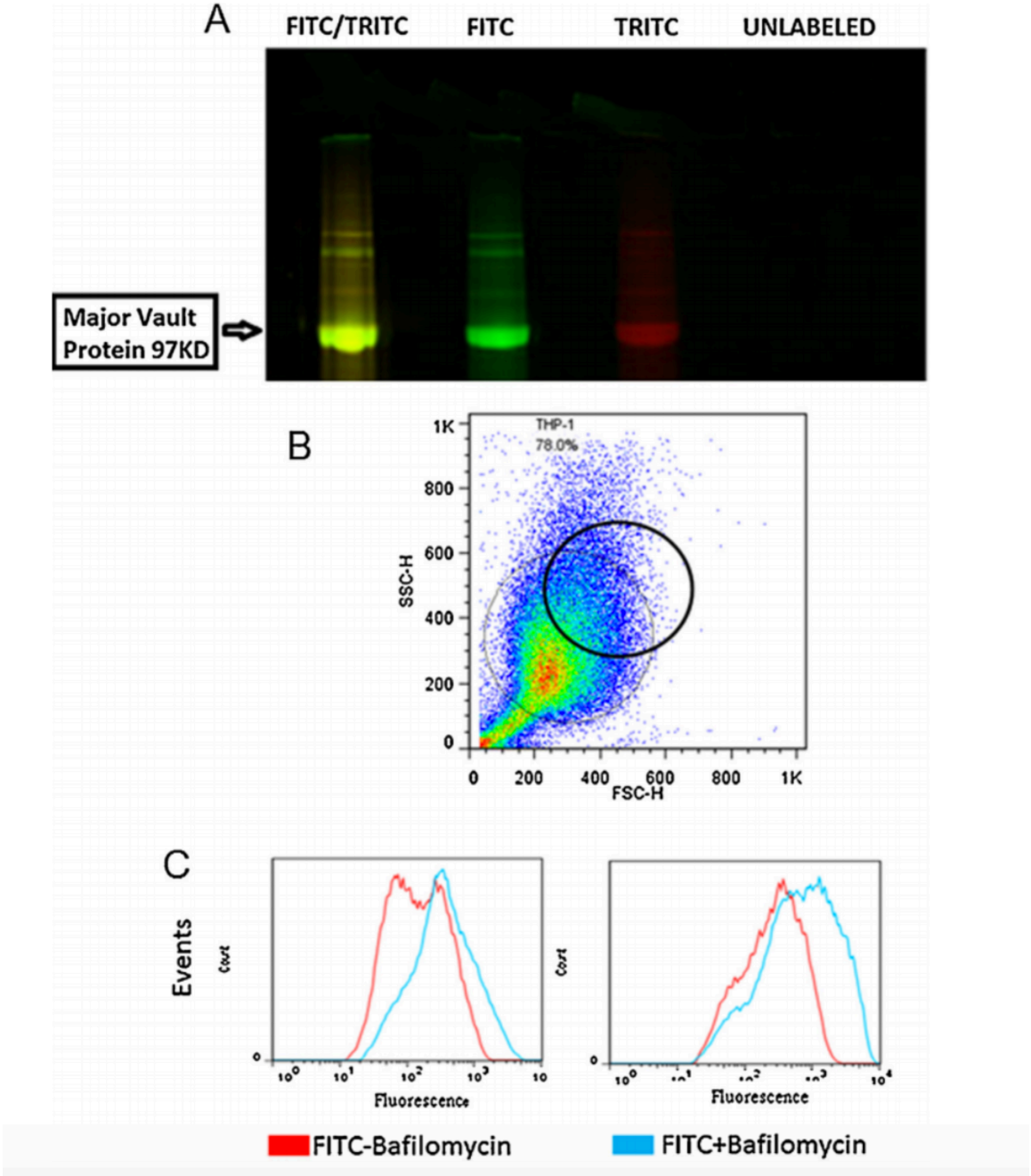

Figure 7 PmpG-1-vaults are internalized into an acidic compartment. (A) PmpG-1-vaults dual-labeled with FITC and TRITC fluorophores and incubated with PMA-activated THP-1 cells. (B) Gating scheme (black circle) showing the dot plot of PMA-activated THP-1 cells after PmpG-1-vaults incubation. FITC can only fluorescence when inside acidified chambers and fluorescence can be modified with bafilomycin which prevents re-acidification of vesicles while TRITC constitutively fluoresces. (C) Overlay histogram of FITC-labeled vault fluorescence ± bafilomycin after 6 hours and 24 hours post vault exposure.

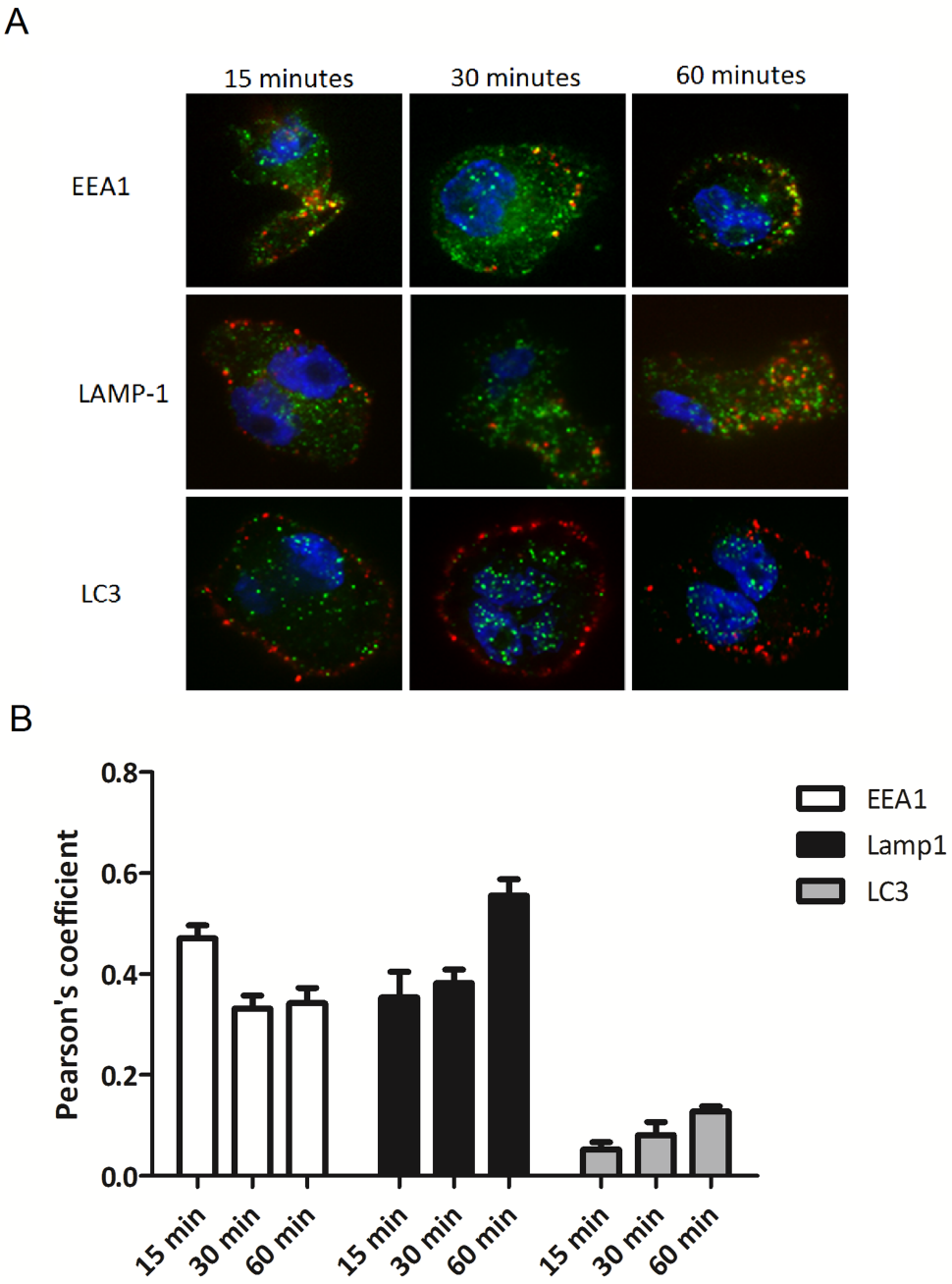

Figure 8 Uptake of PmpG-1-vaults and colocalization within the endocytic pathway. (A) THP-1 cells were grown on 18 mm glass cover slips and treated with 30 g of DyLight 650 labeled PmpG-1-vaults for 15, 30, and 60 minutes and imaged by confocal microscopy. For immunofluorescence staining, THP-1 cells were reacted with anti-EEA1 mouse mAb, anti-Lamp1 mouse mAb, or anti-LC3 mouse mAb followed by Alexa Fluor 488-conjugated goat anti-mouse to identify endocytic compartments. (B) Colocalization of PmpG-1-vaults within each compartment was determined by calculation of the Pearson's correlation coefficient of the red and green channels using ImageJ..

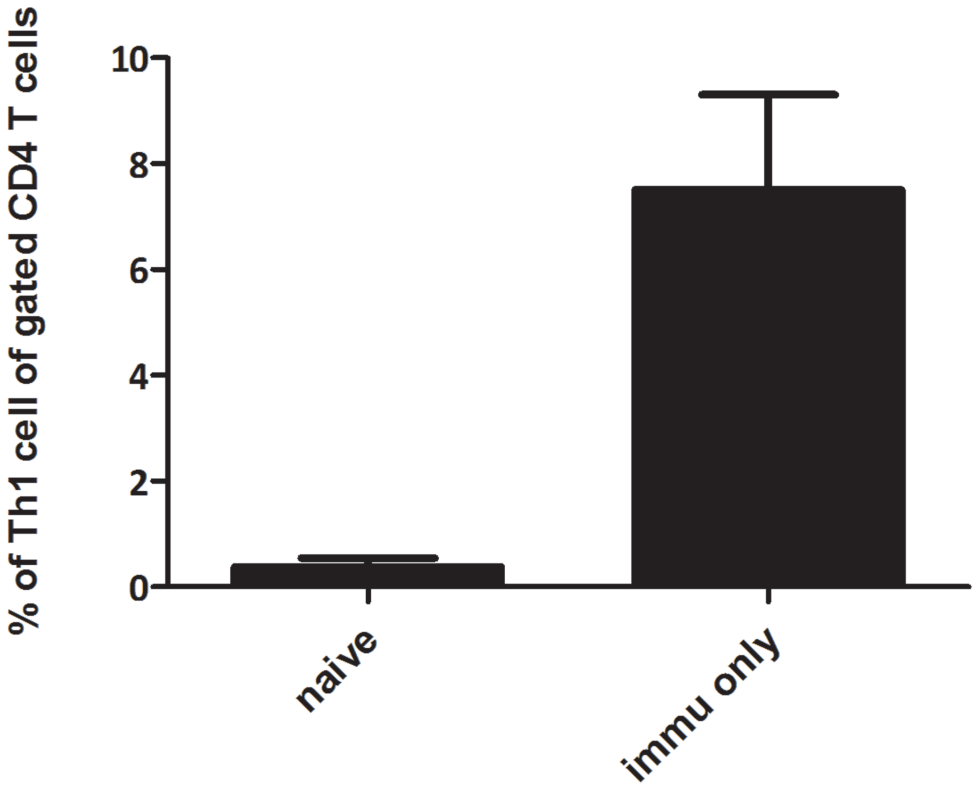

Figure 9 PmpG-1-vaults immunization induces a cellular immune response in vivo. Spleen cells were harvested from naïve mice as well as mice immunized with PmpG- 1-vaults containing a total of 15 g PmpG-1 peptide, 7 days after challenge. Bars indicate percentage of CD3+CD4+IFN+ (Th1) cells out of CD4+ cells following in vitro stimulation with PmpG-peptide (mean % ± SEM). n = 4, $p < 0.001$ by Student's t-test.

3.5 Chlamydia vaults activate canonical and non-canonical inflammasomes

Over the past decades, four different inflammasomes, namely NLRP1, NLRP3, NLRC4, and AIM2 have been identified and characterized. They are classified into canonical inflammasome pathways given their concurrence on the mechanism of caspase-1 activation. However, until very recently does it appear that the pathways leading to caspase-1 activation in response to microbial signals are more complex than previously thought. The caspase-11 may act as an alternative upstream molecule of caspase-1, therefore constitutes a non-canonical mechanism for caspase-1 activation. Accordingly, this pathway can stimulate both caspase-1 dependent and independent production of IL-1β and IL-18. The human orthologs of murine caspase-11 are caspase-4 and caspase-5. To examine whether caspase-4/5 are involved in IL-1β production in THP-1 cells in response to chlamydia-vaults, we applied caspase inhibitors that selectively block caspase-1, -4, and -5. While chlamydia-vaults induced considerable IL-1β secretion in THP-1 cells, this secretion was efficiently blocked by inhibitors of caspase-1, caspase-4 (YVAD, Biovision), and caspase-5 (WEHD, Biovision), used either alone or in combination (Fig.10A). Likewise, the secretion of mature caspase-1 was also hampered under the same conditions (Fig.10B). The fact that both IL-1β and caspase-1 secretion were blocked by caspase-4, 5 inhibitors strongly indicates that non-canonical inflammasomes were also involved in caspase-1 activation by chlamydia-vaults. Recently, it was shown that the murine caspase-11 and human caspase-5 are pathogen recognition receptors for cytosolic LPS. We therefore examined the activation of non-canonical inflammasomes by measuring activation of human caspase-4 in PMA- or LPS-primed THP-1 cells (Fig.10C). Similarly to LPS-induced caspase-4 activation, chlamydia-vaults also stimulated caspase-4 activation, which could be inhibited in the presence of caspase-5 inhibitor (Fig.10C). To our best knowledge, this is the first observation that chlamydia-vaults or nanoparticles of any kind could activate non-canonical inflammasomes. Therefore, we hypothesize that a full protection provided by chlamydia-vaults *in vivo* requires the activation of both canonical and non-canonical inflammasomes (Fig.12).

Another non-canonical inflammasome identified recently was the caspase-8 dependent inflammasome. Our results showed that IL-1β secretion induced by chlamydia-vaults was inhibited when caspase-8 and Syk inhibitor were applied (Fig.11A). However, caspase-1 secretion was not affected by caspase-8 inhibitor comparing to Syk inhibitor, which suggest that caspase-1 secretion was caspase-8 independent (Fig.11B).

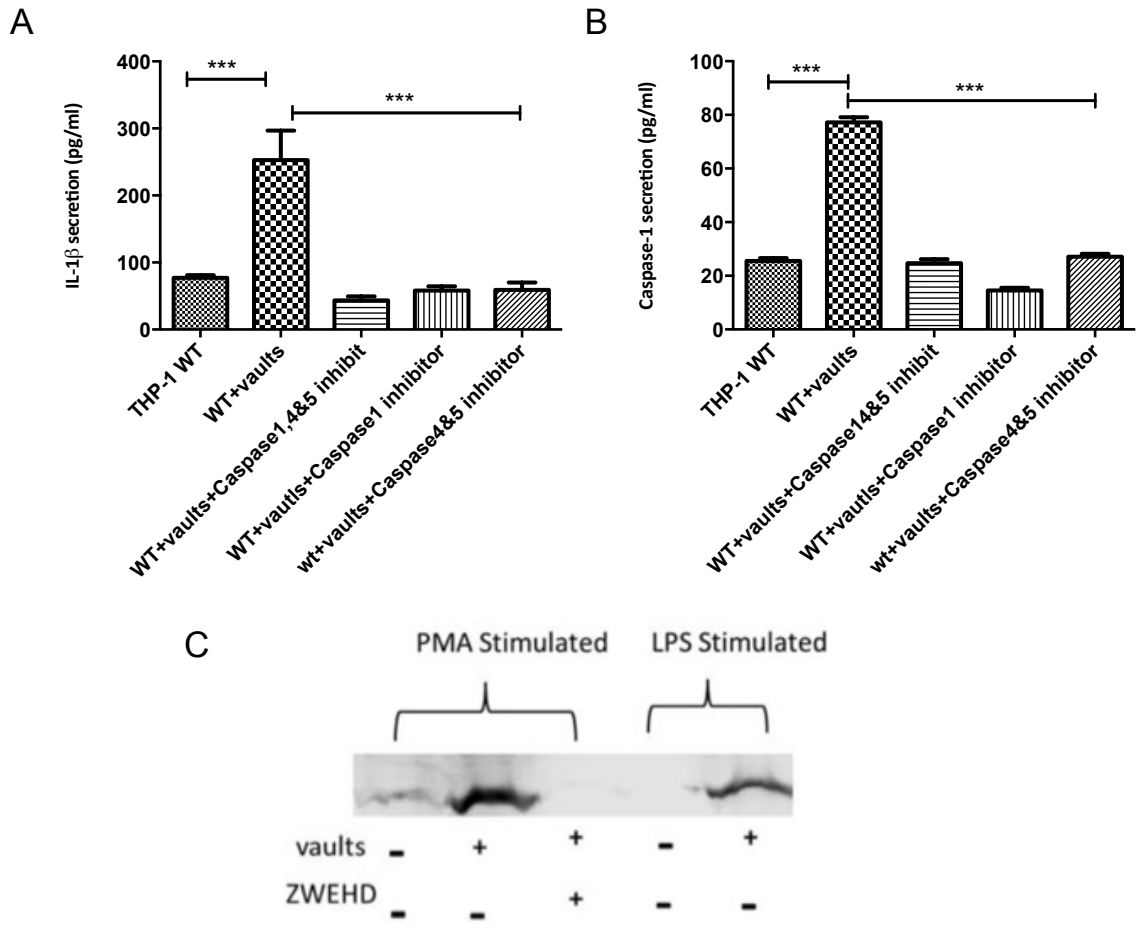

Figure 10 Chlamydia-vaults activate non-canonical caspase-4&5 inflammasome. THP-1 cells were incubated in RPMI media in various conditions as shown above. (A) IL-1β was measured in triplicates by ELISA kit and (B) Caspase-1 was measured in triplicates by ELISA kit. (C) Activated caspase-4 was detected by western blot. Data are collected from at least 3 independent experiments. Error bars represent ±SD, and Student's t test was conducted. N.D (not detected), n.s (not significant), ***P < 0.001

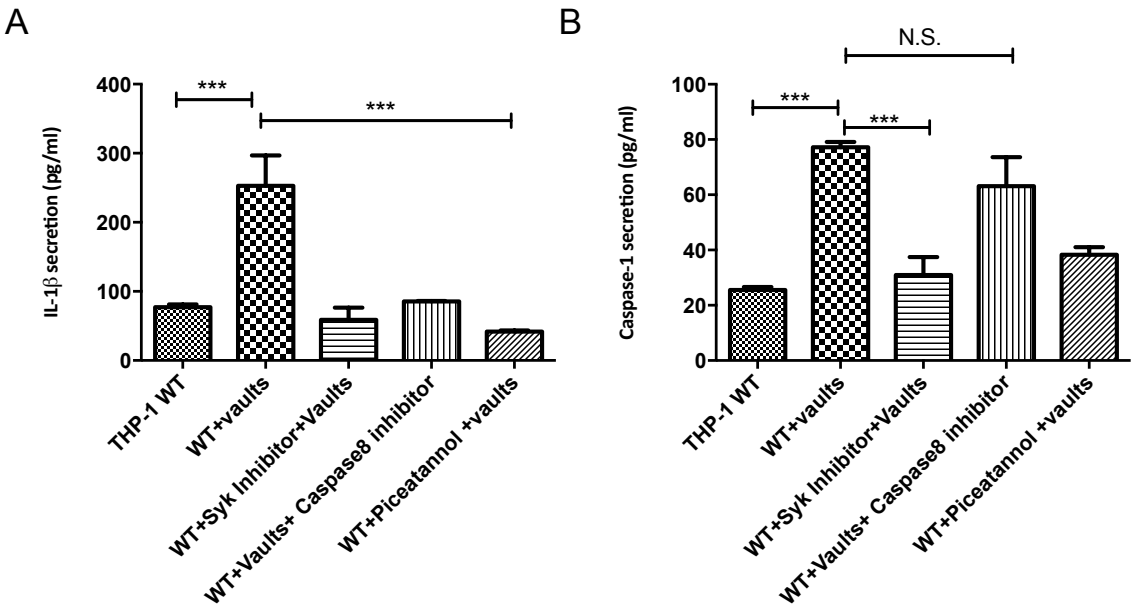

Figure 11 Caspase-8 inhibitor could decrease chlamydia-vaults activated IL-1β secretion but not the caspase-1 secretion. THP-1 cells were infected with Chlamydia-vaults with inhibitors. (A)-(B) IL-1β and caspase-1secretion was analyzed by ELISA. Data are collected from at least 3 independent experiments. Error bars represent ±SD, and Student's t test was conducted. N.D (not detected), N.S (not significant), ***P < 0.001.

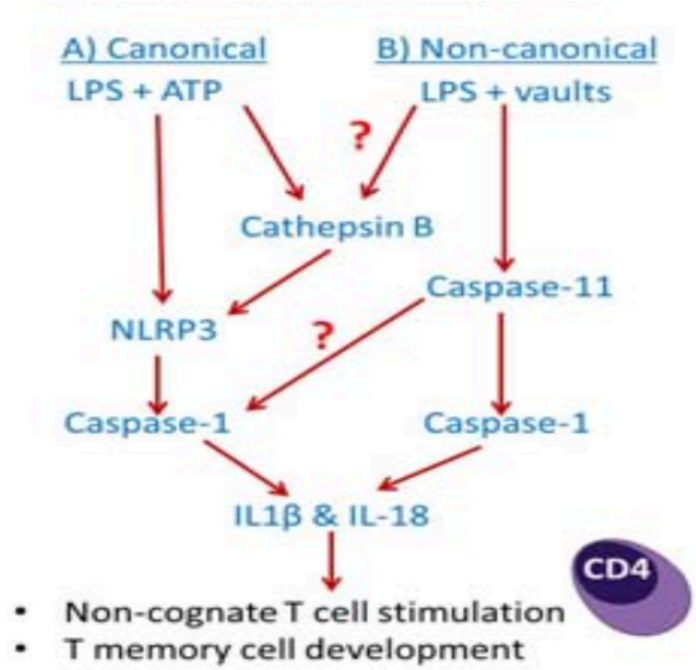

Figure 12 Model of the effect of vault influence on activation.

3.6. Vaults are important for inflammasome induction

Previous *in vitro* work showed that vaults harboring Chlamydia antigen could stimulate innate immune response by activating the NLRP3 inflammasome. To further understand how vaults impact a chlamydial genital infection, we infected MVP KO mice that are deficient in endogenous vaults. MVP KO mice were infected intravaginally with *C.muridarum* following a 7-day treatment with progesterone. We found that MVP KO mice displayed a statistically greater bacterial burden in the genital tract after infection than the WT mice (Fig.13A).

A.

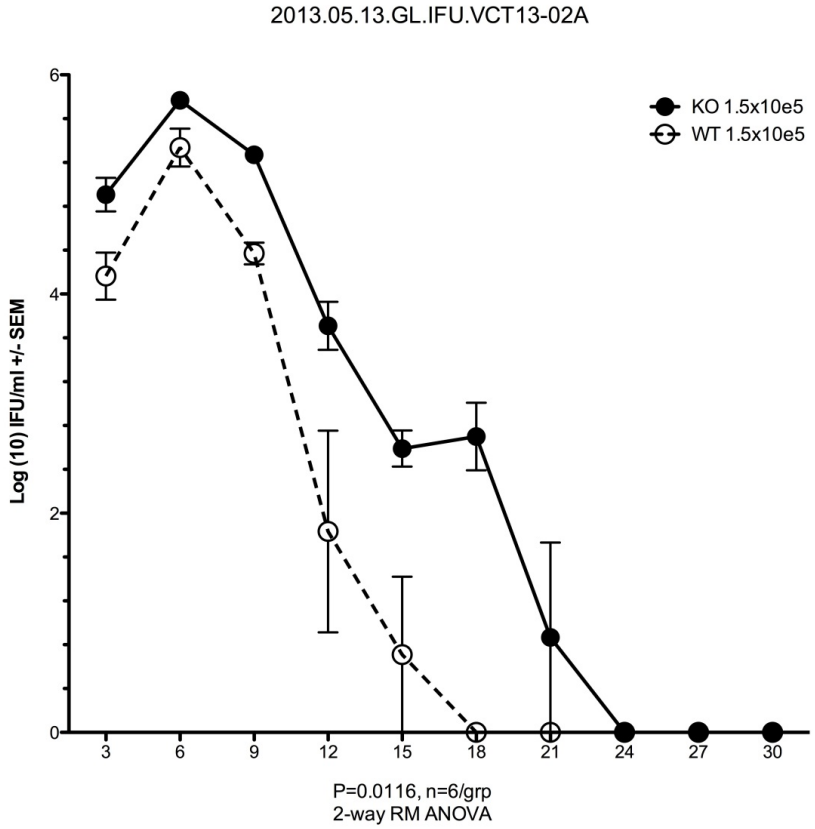

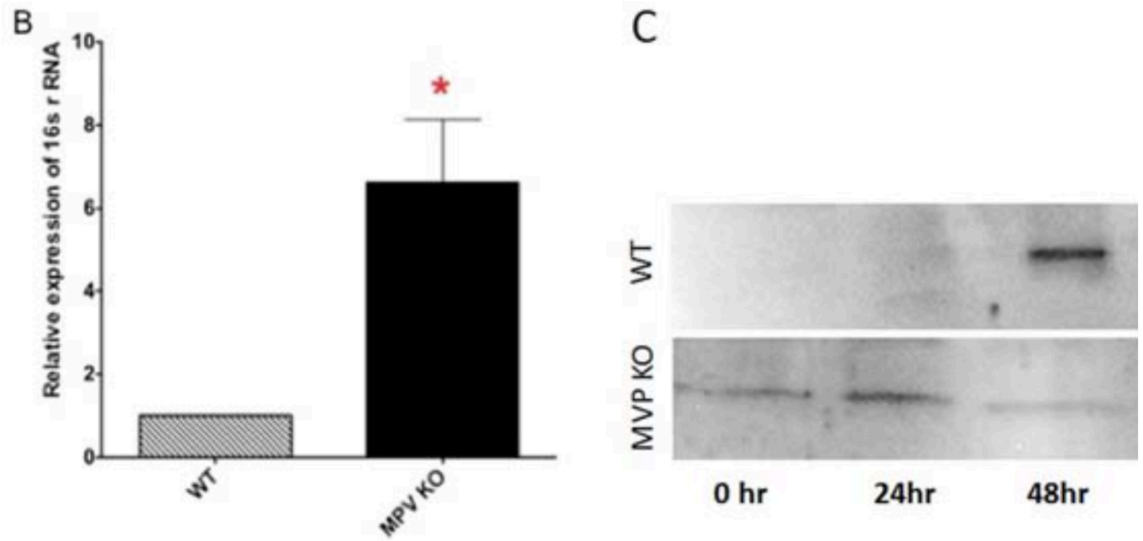

Figure 13 Vaults are required for inflammasome activation. A. Results of bacterial burden from vaginal swabs following infection. *P<0.001 by two way ANOVA, n=6/group. B. Relative levels of C. trachomatis 16s rRNA after 48 hours of infection with MOI 1 of *C. trachomatis* in MEF cells from WT and MVP KO mice. C. Western blot of activated caspase-1 following infection with MOI 1 of *C. trachomatis* in MEF from WT or MVP KO mice.

Mouse embryonic fibroblasts (MEFs) from both MVP KO and WT mice were also infected *in vitro* with *C.m* for 48 hours. As expected, MEFs from MVP KO mice accumulated more than 5 fold of *C.m* than the WT mice as measured by *C.m* 16S rRNA levels (Fig.13B). Moreover, *C.m* infection of MEFs from WT mice induced a high level of mature caspase-1 after 48 hours, indicating the activation of inflammasome. In contrast, infection of MEFs from KO mice failed to induce caspase-1 production, indicating that vaults are important for inflammasome induction (Fig.13C).

Chapter 4. Discussion and future perspectives of chlamydia-vaults project:

Vaccines that prevent significant infection of the female genital tract are essential to reduce the incidence of PID following *C. trachomatis* infection. We have shown that vaults containing a chlamydial protein (MOMP) markedly reduces infection early after infection, suggesting that the self-adjuvanting vault vaccine activates innate immunity while not elicits excessive inflammation as measured by TNF-α production [74]. In this study, we characterized the innate immune response from the perspective of inflammasome activation. The results demonstrate that incubation of PMA-primed THP-1 cells with PmpG-1-vaults can activate caspase-1 and stimulate IL-1β secretion through a process requiring the NLRP3 inflammasome. We found that the cathepsin B inhibitor CA-074 Me could partially inhibit this process. Interestingly, when internalized PmpG-1-vaults were visualized in cells, we found that the vaults co-localized with lysosomes at early time points post-entry. Moreover, the lysosomal permeabilization assay demonstrated that the PmpG-1-vaults localized in acidic compartments at early time points, but were subsequently transferred to an environment with neutral pH. Once lysosomes are ruptured, they release proteases such as cathepsin B, which have been previously shown to activate the NLRP3 inflammasome.

Syk also modulates vault-induced inflammasome activation. While the mechanism for this dependence is not yet known, the Syk kinase is known to be recruited into lipid rafts when phagosomes form [83]. It has also been proposed that MVP is involved in intracellular transport and is concentrated in lipid rafts [84]. Given that vaults are phagocytosed by cells during incubation, we speculate that PmpG-1-vaults might enter the cells though lipid rafts and then interact with Syk kinase and, simultaneously, lysosomes, in order to activate the NLRP3 inflammasome. Alternatively, the chlamydia-vaults were engineered with a 33 amino acid–peptide called the “Z” domain. This peptide was derived from a staphylococcal-binding domain that can bind the Fc portion of IgG at a site distinct from the binding site for the Fc receptor (FcR). It has also been previously shown that vaults with a “Z” domain increase binding of mouse IgG [74]. We expected that these vaults would be internalized through the FcR, which also stimulates the Syk pathway [84]. Further studies should elucidate the mechanisms whereby chlamydia-vaults stimulate Syk- and cathepsin B-dependent NLRP3 inflammasome activation.

Taken together, these findings support a model whereby *in vivo* administered vault-vaccines are phagocytosed by antigen presenting cells as we have shown *in vitro* using BMDC [85]. Following internalization, we showed that incubation of monocytes with chlamydia-vaults could activate caspase-1 and stimulate IL-1β secretion through a process requiring the NLRP3 inflammasome. Inhibitors of the lysosomal protease, cathepsin B, prevented inflammasome activation, implying that lysosomal disruption likely plays a role in caspase-1 activation. This interpretation is consistent with the observation that the chlamydia-vaults are internalized through a pathway that is transiently acidic and leads to destabilization of lysosomes. Chlamydia-vault interaction within cells are unique from other reported activators of NLRP3 inflammasomes, in that Syk was also shown to be involved in PmpG-1-vault-induced inflammasome activation, which may be due to vault interactions with lipid rafts. Vault vaccines can also be engineered to induce specific adaptive immunity, as we have shown here that immunization of mice with chlamydia-vaults induces generation of chlamydia-responsive $CD4^+$ cells immune cells. Vaults can also be engineered to deliver drugs and promote anti-tumor responses [74, 77, 78]. These studies define vault-vaccines as unique among other vaccines that induce NLRP3 inflammasomes, such as alum, as they are also able to induce specific marked T cell responses against antigens incorporated in the vault body.

Chapter 5. Results: Activation of the NLRP3 inflammasome by Chlamydia in Gingival Epithelial Cells.

Chlamydia pneumoniae (*C.pn*) is an airborne chlamydial species responsible for human respiratory infection. It is also associated with atherosclerosis, coronary heart disease, and hyperlipidemia.[50] *C.pn* needs to persist within the infected tissues for periods in order to stimulate a chronic inflammatory response. *C.pn* has been shown to disseminate systemically from the lungs through infected peripheral blood mononuclear cells to localize in arteries where it may infect endothelial cells, vascular smooth muscle cells, monocytes/ macrophages and promote inflammatory atherogenous process. [51,53]. Interestingly, we questioned where *C.pn* comes from. It has recently been shown to be a new member of the human oral microbiota. One clinical case reported that *C.pn* was detected in human dental plaque and may relate to periodontitis. The first line of defense against microbial infection lies in the tissues such as skin and oral mucosa. Human gingival epithelial cells (GECs) represent the prominent component of the oral cavity and are the common targets for periodontal-pathogen infection. Therefore, we hypothesize that *C.pn* adheres to gingival epithelial cells and infects them leading to inflammation, which may further contribute to oral diseases or lung infections.

5.1 *C. pneumoniae* infects human gingival epithelial cells

In order to determine the infection ability of *C.pn* in oral environment, we established GEC cells as a physiologically relevant model to study oral infection and diseases. GEC cells were infected with *C.pn* for four days and stained for cell nucleus (shows blue) and *C.pn* (shows green). Immunofluorescence microscopy results showed that the lung disease pathogen *C.pn* could infect human gingival epithelial cells during four days (Fig.14A). At the meantime, we found that the inclusions formed in GEC occurred at later time points from around 72 hours to 96 hours, while in lung epithelial cells it was ranged from 48 hours to 72 hours. Therefore we questioned if the infection efficiency differs in different cell types. We tested the infection of *C.pn* in three cell lines including GECs, HeLa, and A459. A459 cells are lung carcinoma epithelial cells and are considered as an ideal model for Chlamydia infection and disease development. With the same multiplicity of infection of *C.pn*, GECs displayed the same level of infection efficiency as compared to HeLa and A459 cells (Fig.14B). Real-time PCR analysis of the *C.pn* 16S RNA expression level showed that *C.pn* attached the cells on the first day and infected on the second day. The cells exhibited a great bacterial burden on day 2 and limited growth during the infection. The *C.pn* 16S RNA expression level declined on day 5 when elementary bodies exited the host through lysis or extrusion (Fig.14C). Therefore, we conclude that human lung pathogen *C.pn* could infect GEC cells.

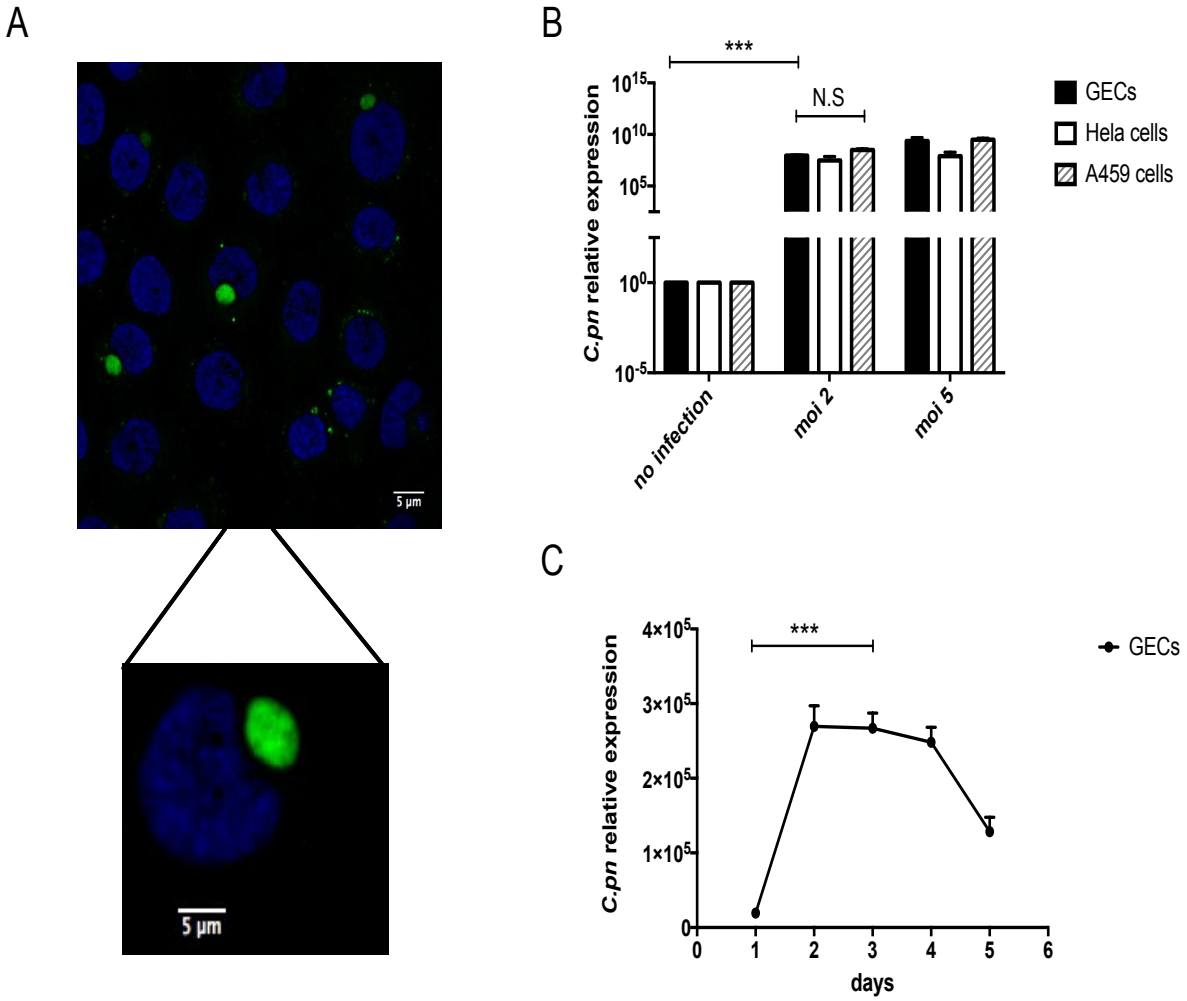

Figure 14 Infection of human gingival epithelial cells *C. pneumoniae*. (A). GEC cells were grown on 18 mm glass cover slips and treated with *C.pn* in MOI 5 for four days and imaged by confocal microscopy. For immunofluorescence staining, GEC cells were reacted with either Hoechst endocytic compartments (Bio-rad), anti- *C.pn* antibody. Nuclear was showed in blue and *C.pn* showed in green. (B) *C.pn* infect efficiency was confirmed in Q-PCR compared with Hela cells and A459 cells in day 2, MOI 5. (c) *C.pn* infection level among 5 days were examined by Q-PCR, *C.pn* 16s RNA was applied to detect infection. Data were collected from 4 independent experiments. Error bars represent ±SD, and Student's t test was conducted. ***P < 0.001.

5.2 Inflammasome is activated during *C.pn* infection of GEC cells model.

Previous studies showed that oral bacterium like *Fusobacterium nucleatum* could induce GEC to overexpress pro-IL-1β therefore leading to IL-1β secretion [86]. Moreover, *C.pn* infection in THP-1 cells was also shown to induce IL-1β secretion [87]. Therefore we sought to examine whether *C.pn* infection could trigger GEC cells to secrete IL-1β. GEC cells were infected with *C.pn* at a MOI of 5 for different time points. To measure the levels of mature IL-1β, Supernatants from infected cells were collected and subjected to ELISA analysis. The results showed that IL-1β secretion from infected cells increased over the 5-day infection period, which reached the peak on day 4. In parallel, the uninfected group did not show a significant change over time (Fig. 15A). As the pro-inflammatory protease caspase-1 is essential for IL-1β secretion [88], we next investigated the role of caspase-1 in *C.pn* induced IL-1β secretion. To this end, we collected the supernatants from both *C.pn* infected and uninfected groups, and the supernatants were concentrated according to the TCA protein precipitation protocol. Western blot analysis showed that the levels of caspase-1 increased from day 1 to day 4. (Fig.15B and C). These observations reason why IL-1β level peaked on day 4, and demonstrate that *C.pn*-induced IL-1β secretion relies on caspase-1 activation.

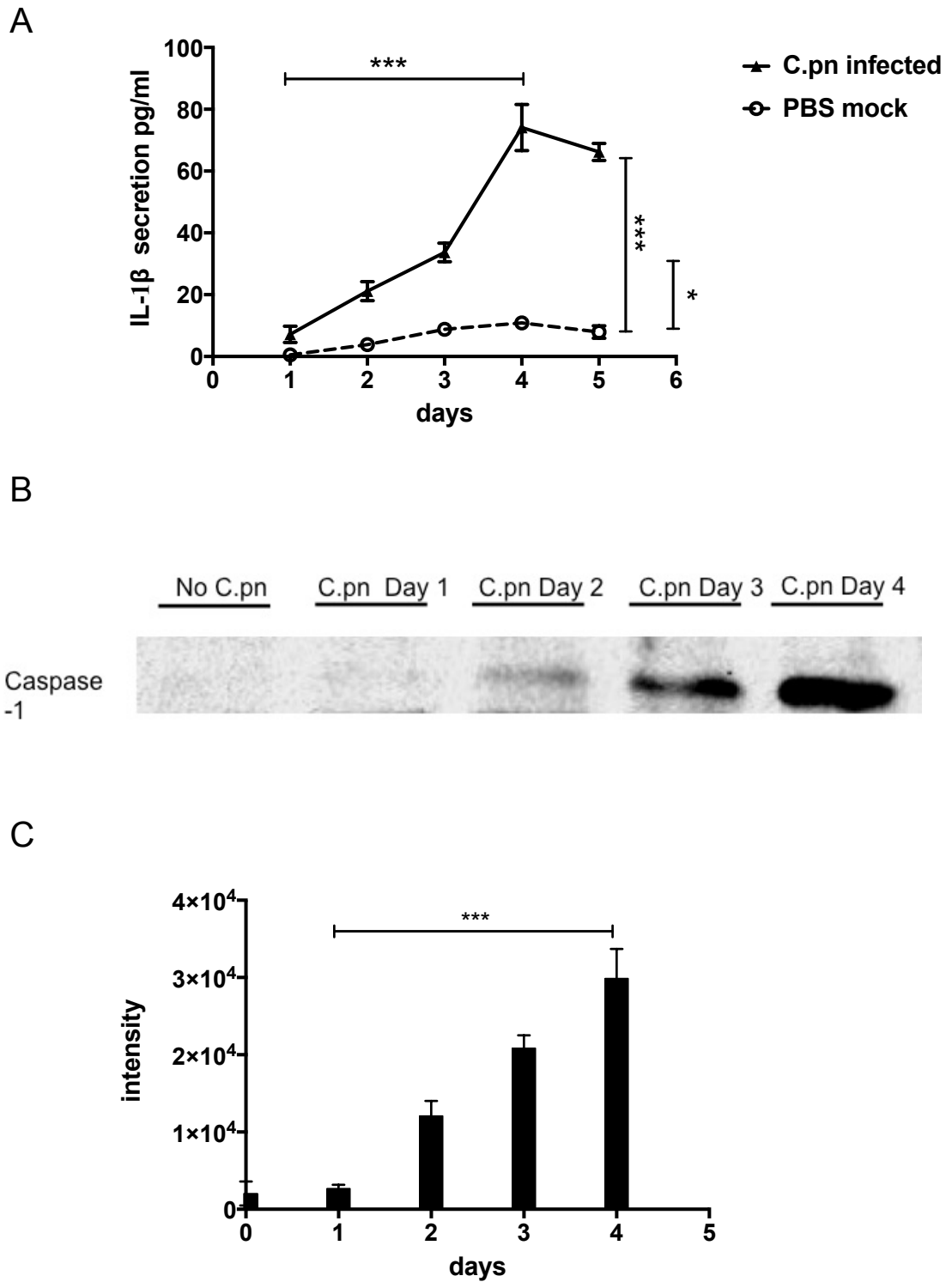

Figure 15 Caspase-1 is activated during C.pn infection in GECs. (A) ELISA measurement for IL- 1β during five days of *C.pn* infection. PBS mock group was applied as a negative control. (B) Caspase-1 secretion was checked with western blot, and the analysis of the caspase-1 western blot was shown in (C) by intensity of each lane. Data were collected from 3 independent experiments. Error bars represent ±SD, and Student's t test was conducted. ***P < 0.001.

5.3 NLRP3 inflammasome is activated in response to *C.pn* infection.

We have shown that *C.pn* infection of GECs could induce inflammasome activation and mature IL-1β and caspase-1 secretion. It is next necessary to determine on which inflammasome it depends. Previous studies showed that sub-gingival bacteria could activate NLRP3 inflammasome in gingival epithelial cells. Moreover, NLRP3 inflammasome was reported as a key player during *C.pn* infection in THP-1 cells. Of note, it was mentioned in the earlier chapter that the inflammasome is a multiprotein oligomer consisting of ASC, NLRs and caspase-1. To interrogate whether caspase-1 secretion in GECs was dependent on NLRP3 inflammasome activation, we silenced NLRP3 gene expression by using lentivirus, and the knockdown efficiency was tested by qPCR. (Fig.16A). One monoclonal cell line with a significant knockdown effect was selected for later research. The knockdown cells were cultured and infected with *C.pn* under the same conditions as the wile type cells and the control group. Supernatants were subsequently collected and subjected to Western blot analysis. Results showed that caspase-1 secretion was blocked in NLRP3 KD cells as compared with the wild-type cells and the control group. (Fig.14B and C)

ASC is a key component of the NLRP3 inflammasome. It recruits and activates caspase-1 , which in turn maturates cytokines such as IL-1β. Recent studies showed that upon NLRP3 inflammasome activation, ASC accumulates as specks and might be released to the extracellular space. These ASC specks and their release were regarded as a hallmark of inflammasome activation. By using immunofluorescence microscopy, we showed that ASC accumulated into speck-like structures in the cytosol on the third day of infection with *C.pn* in GEC cells (Fig.16). Along with the development of inflammation, ASC concentrated in the cytosol and the ASC specks were detected extracellularly on day four and five. Taken together, these results demonstrate that the NLRP3 inflammasome is activated in GECs upon *C.pn* infection.

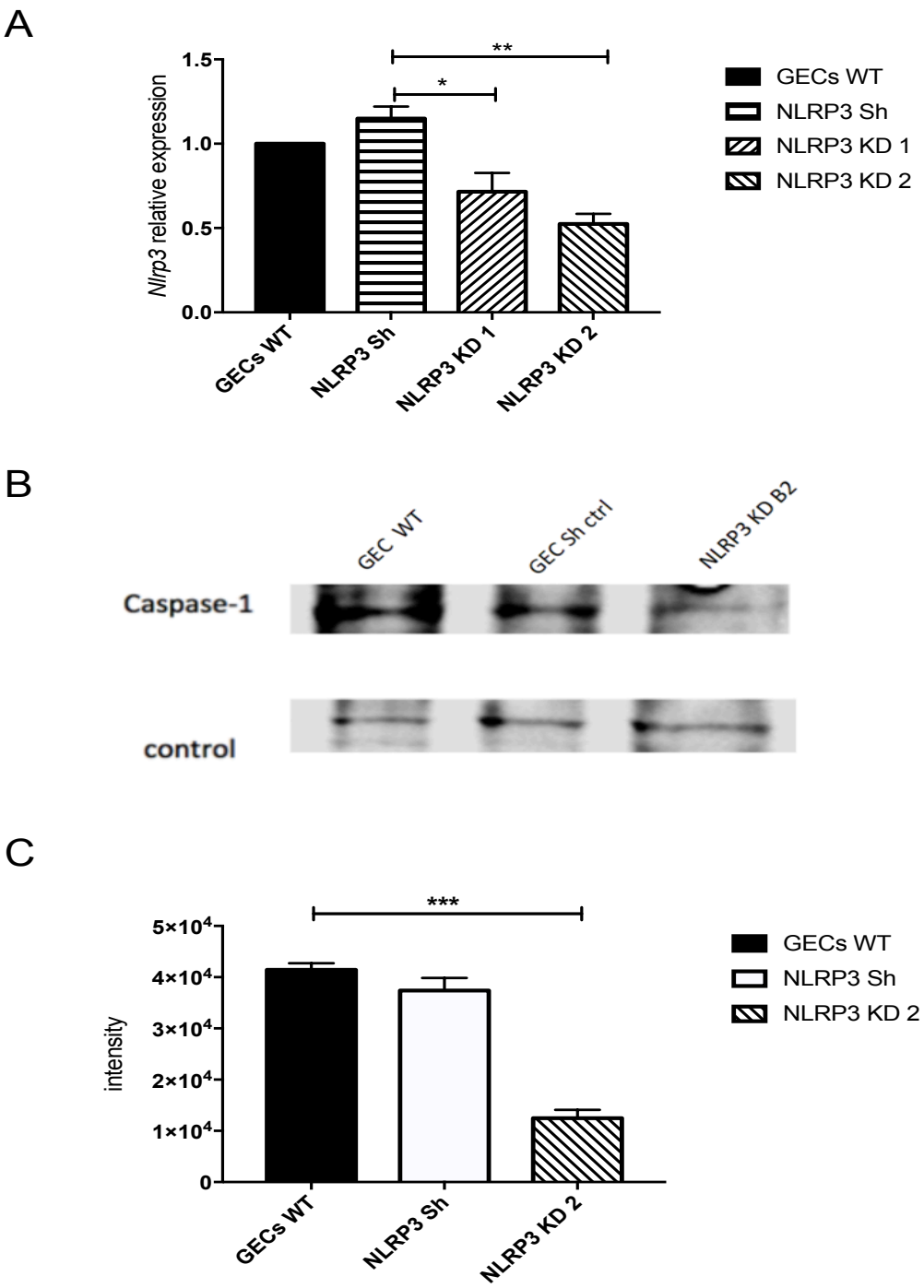

Figure 16 *C.pn*-induced caspase-1 secretion in GECs requires NLRP3. (A) Results of nlrp3 relative expression among wild type cells and sh control and knockdown cells. (B) Results of caspase-1 western blot from supernatant, and the intensity level were showed in (C). Data were collected from 3 independent experiments. Error bars represent ±SD, and Student's t test was conducted. *P<0.5, **P < 0.01, ***P<0.001.

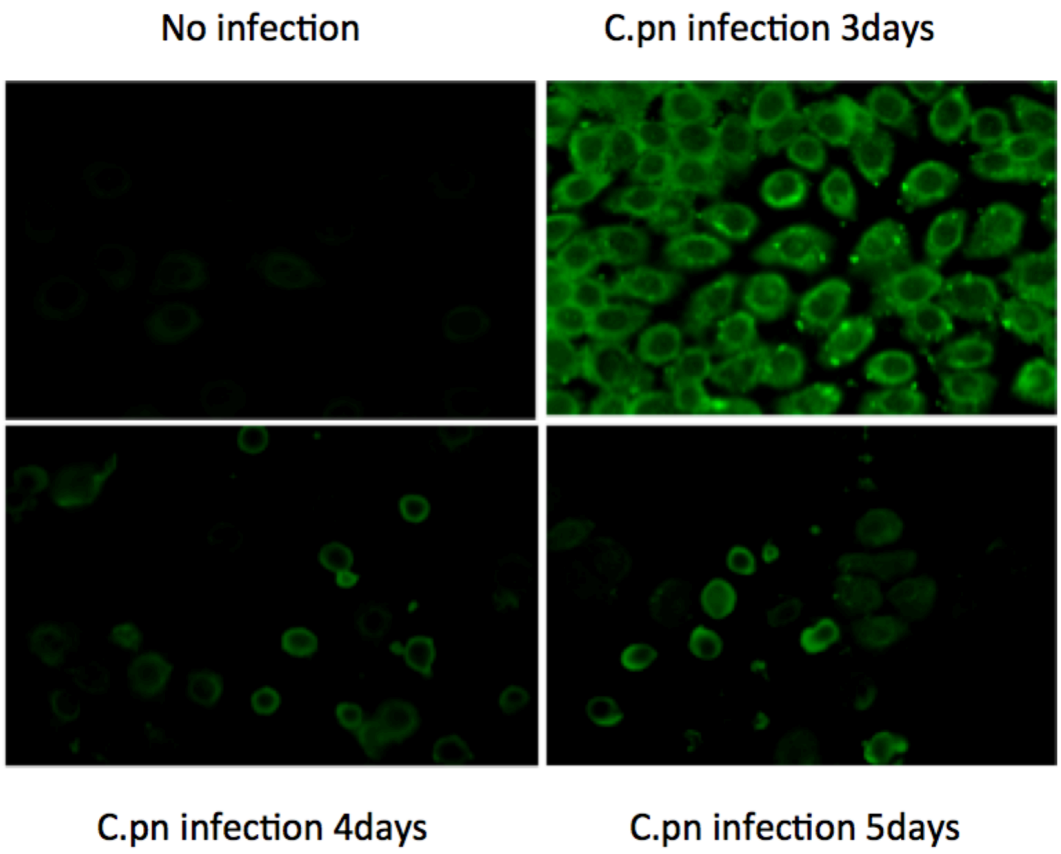

Figure 17 *C.pn*-induced inflammasome activation leads to the formation of ASC. GEC cells were grown on 18 mm glass cover slips and treated with C.pn in MOI 5 and imaged by florescent microscopy. For immunofluorescence staining, GEC cells were reacted with ASC-GFP showing in green.

5.4 *C.pn* is identified in plaque samples from patients with periodontitis.

We have shown that *C.pn* could infect human gingival epithelial cells and induce inflammasome activation *in vitro*. Previous study reported that *C.pn* in oral environment might relate to periodontal disease [89]. To determine whether *C.pn* exists and affects any oral diseases, we collected 40 samples from 10 patients with periodontitis. Subgingival plaque samples from the deepest pocket of each quadrant were collected for analysis. RTF buffer was selected to dissolve and maintain the DNA from the plaque samples. The PCR results turned out to be interesting that most of the samples showed positive for *C.pn* even for the ones from the healthy sites (Fig.16). Considering that bacteria or oral commensals might easily translocate during chewing, it would be reasonable to see that *C.pn* was also detected in healthy sites. The high frequency, 10 out of 10 patients' plaques containing *C.pn,* indicates a potential involvement of *C.pn* infection in the disease progression. However, further experiments should be warranted to illustrate such involvement.

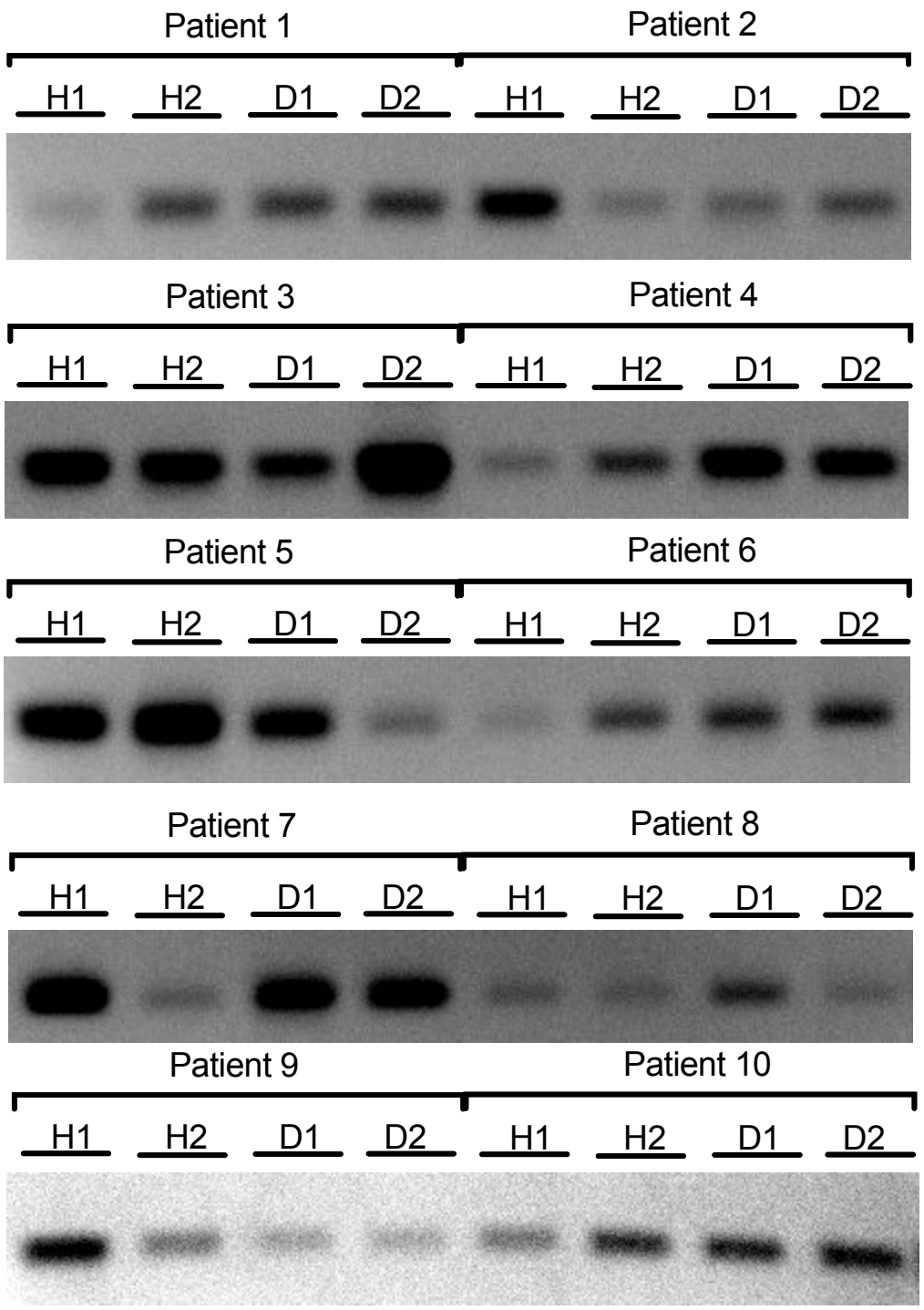

Figure 18 Positive detection of *C.pn* in the plaque samples from patients with periodontitis. Gel electrophoresis of PCR products, suing primers for C.pn 16sRNA. 10 patients' plaque samples were used and showed *C.pn* positive for existing. Pure *C.pn* strains were used as a positive control. (not shown here). Experiments were repeated at least 3 times and the represented figure showed.

5.5 SREBPs are associated with C.pn induced NLRP3 inflammasome.

Sterol regulatory element binding proteins (SREBPs) have been reported to associate with NLRP3 inflammasome in atherosclerosis. SREBPs also promote cell survival during bacteria infection by facilitating membrane repair, requiring caspase-1 activation. Periodontitis and *C.pn* infection are considered as two independent risk factors for cardiovascular diseases due to fatty acid imbalance [100]. Therefore, it is important and necessary to investigate whether SREBPs level is affected by *C.pn* infection in GEC cells. Interestingly, we found that *C.pn* infection induced significantly lower level of activated SREBP-1 in NLRP3 knockdown cells compared to the wild-type cells (Fig.16). This impaired presence of SREBP-1 might control cholesterol and lipid biosynthesis.

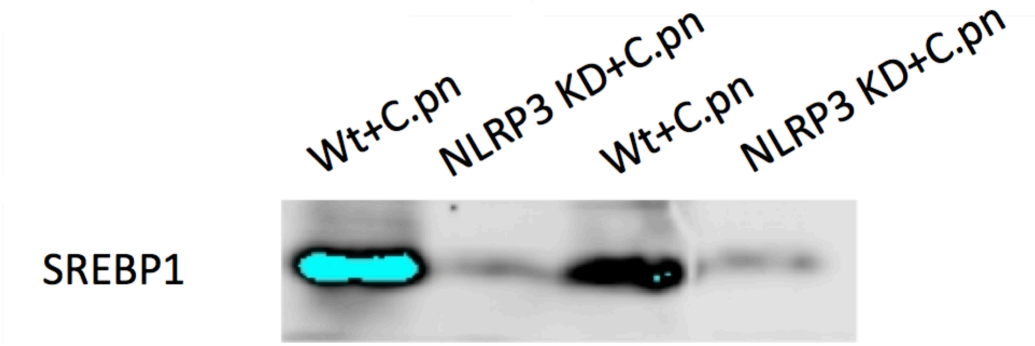

Figure 19 Western blot of activated SREBP1 following infection with MOI 5 of *C. pneumoniae* in GEC wild type or knockdown cells.

Chapter 6. Discussion and future perspectives of *C.pn* project

C.pneumoniae like other chlamydia species are intracellular pathogens and usually infect epithelial mucosa and develop a biphasic infection cycle [57]. In this study, we showed that *C.pn* could infect human gingival epithelial cells and develop its infection cycle in around three days. We confirmed this infection by using both confocal microscopy and quantitative PCR.

Previous studies showed that the proinflammatory cytokine IL-1β is an important mediator during host defense against microbial organisms [90]. Crucially, the level of IL-1β is tightly controlled since it induces chronic infections and damages tissues if being inappropriately released. When properly released, IL-1β activates inflammation to protect the host [91, 92]. IL-1β secretion occurs when other Chlamydia species infect human monocytes and macrophages and activate inflammasome activation. We examined IL-1β secretion level in this study and found that it peaked on day four. Activated caspase-1 is required for processing pro-IL-1β into IL-1β during inflammation [93-95]. Our results on caspase-1 release were consistent with IL-1β secretion, both of which increased after infection and reached the peak value on day 4. NLRP3 but not NLRC4 inflammasome was reported to be activated during *C.pn* infection in murine model [96]. And NLRP3 inflammasome was also studied in GECs with oral diseases infection [97]. We confirmed the involvement of NLRP3 inflammasome using the NLRP3 KD cells and found that both the IL-1β level and caspase-1 secretion were impaired. NLRP3 inflammasome is a multiprotein complex, in which its adaptor protein ASC was reported to concentrate once inflammasome is activated [98-100]. We did observe that ASC was concentrated during infection; however, whether ASC was released out of cells needs to be further determined.

It might be surprising to witness that lung pathogens infect oral epithelial cells and activate inflammasome. We questioned whether this infection and inflammasome activation occur inevitably and how it relates to oral diseases. Periodontitis is one of the major concerns among oral diseases [101]. CDC reported that half of the American adults have periodontal disease. Its symptoms range from simple gum inflammation to serious damage to soft tissue and teeth loss. Our clinical results showed that periodontal patients had a higher risk to be infected by *C.pn*. Whether inflammasome activation by *C.pn* infection in patients aggravates or mitigates the diseases warrants further research.

SREBP was reported to associate with caspase-1 during bacterial infection and could be up-regulated by caspase-1 [102]. Once activated, SREBP is translocated into the nucleus. This lipid metabolism in turn promotes cell survival and repair [102]. We extracted the nucleus from the cell pellet and found that the SREBP levels from the wild-type cells were higher than that from the NLRP3 knockdown cells during *C.pn* infection. These results indicate that caspase-1 or NLRP3 inflammasome triggers SREBP activation.

In agreement with this event, *in vivo* study showed that dysregulation of SREBP may contribute to inflammation in atherosclerosis [103]. Interestingly, *C.pn* is identified as

the only chlamydia species that exerts atherosclerosis-effect. The activation of NLRP3 inflammasome by *C.pn* is involved in the acceleration of atherosclerosis [96]. Moreover, clinical cases collected in the last two decades corroborated that periodontitis is a risk factor to atherosclerosis [104, 105]. However, the mechanism of which remains elusive. Whether *C.pn* related periodontitis contributes to atherosclerosis requires further investigation. Taken together, these findings highlight the importance of the inflammation induced by *C.pn* in oral environment.

In this study, we demonstrated that caspase-1 represents a key component in *C.pn* infection that leads to pro-IL-1β processing and lipid metabolism regulation. We have previously showed that *C.t* could also activate non-canonical inflammasomes such as caspase-4/5. For future studies, whether *C.pn* infection of GECs also induces caspase-4/5 pathways needs to be determined.

In conclusion, our work not only broadens the current knowledge on the oral epithelial cell response to *C.pn* infection and the pathogenesis associated with it, but also sheds light on a plausible correlation of lung pathogens with oral diseases. This provides novel insight into the etiology and therapeutic approaches to oral diseases.

References

1. Charles A. Janeway, J.a. and R. Medzhitov, *INNATE IMMUNE RECOGNITION.* Annual Review of Immunology, 2002. **20**(1): p. 197-216.
2. Gordon, S., *Pattern Recognition Receptors: Doubling Up for the Innate Immune Response.* Cell, 2002. **111**(7): p. 927-930.
3. Medzhitov, R. and C.A. Janeway Jr, *Innate Immunity: The Virtues of a Nonclonal System of Recognition.* Cell, 1997. **91**(3): p. 295-298.
4. Thompson, M.R., et al., *Pattern Recognition Receptors and the Innate Immune Response to Viral Infection.* Viruses, 2011. **3**(6): p. 920.
5. Tang, D., et al., *PAMPs and DAMPs: signal 0s that spur autophagy and immunity.* Immunological Reviews, 2012. **249**(1): p. 158-175.
6. Iwasaki, A. and R. Medzhitov, *Toll-like receptor control of the adaptive immune responses.* Nat Immunol, 2004. **5**(10): p. 987-995.
7. Takeda, K. and S. Akira, *Toll-like receptors in innate immunity.* International Immunology, 2005. **17**(1): p. 1-14.
8. Takeda, K., T. Kaisho, and S. Akira, *TOLL-LIKE RECEPTORS.* Annual Review of Immunology, 2003. **21**(1): p. 335-376.
9. Gilmore, T.D., *Introduction to NF-[kappa]B: players, pathways, perspectives.* Oncogene, 0000. **25**(51): p. 6680-6684.
10. Khanjani, S., et al., *NF-κB regulates a cassette of immune/inflammatory genes in human pregnant myometrium at term.* Journal of Cellular and Molecular Medicine, 2011. **15**(4): p. 809-824.
11. Duncan, J.A., et al., *Cryopyrin/NALP3 binds ATP/dATP, is an ATPase, and requires ATP binding to mediate inflammatory signaling.* Proceedings of the National Academy of Sciences of the United States of America, 2007. **104**(19): p. 8041-8046.
12. Faustin, B., et al., *Reconstituted NALP1 Inflammasome Reveals Two-Step Mechanism of Caspase-1 Activation.* Molecular Cell, 2007. **25**(5): p. 713-724.
13. Kanneganti, T.-D., *Central roles of NLRs and inflammasomes in viral infection.* Nat Rev Immunol, 2010. **10**(10): p. 688-698.
14. Harton, J.A., et al., *Cutting Edge: CATERPILLER: A Large Family of Mammalian Genes Containing CARD, Pyrin, Nucleotide-Binding, and Leucine-Rich Repeat Domains.* The Journal of Immunology, 2002. **169**(8): p. 4088-4093.
15. Inohara, N., et al., *Human Nod1 Confers Responsiveness to Bacterial Lipopolysaccharides.* Journal of Biological Chemistry, 2001. **276**(4): p. 2551-2554.
16. Ogura, Y., et al., *Nod2, a Nod1/Apaf-1 Family Member That Is Restricted to Monocytes and Activates NF-κB.* Journal of Biological Chemistry, 2001. **276**(7): p. 4812-4818.
17. Proell, M., et al., *The Nod-Like Receptor (NLR) Family: A Tale of Similarities and Differences.* PLoS ONE, 2008. **3**(4): p. e2119.

18. Ting, J.P.Y., S.B. Willingham, and D.T. Bergstralh, *NLRs at the intersection of cell death and immunity.* Nat Rev Immunol, 2008. **8**(5): p. 372-379.
19. Dinarello, C.A., *Interleukin 1 and interleukin 18 as mediators of inflammation and the aging process.* The American Journal of Clinical Nutrition, 2006. **83**(2): p. 447S-455S.
20. Ogura, Y., F.S. Sutterwala, and R.A. Flavell, *The Inflammasome: First Line of the Immune Response to Cell Stress.* Cell. **126**(4): p. 659-662.
21. Martinon, F. and J. Tschopp, *Inflammatory caspases and inflammasomes: master switches of inflammation.* Cell Death Differ, 2006. **14**(1): p. 10-22.
22. Allen, I.C., et al., *The NLRP3 Inflammasome Mediates in vivo Innate Immunity to Influenza A Virus through Recognition of Viral RNA.* Immunity, 2009. **30**(4): p. 556-565.
23. Muñoz-Planillo, R., et al., *A Critical Role for Hemolysins and Bacterial Lipoproteins in Staphylococcus aureus-Induced Activation of the Nlrp3 Inflammasome.* Journal of immunology (Baltimore, Md. : 1950), 2009. **183**(6): p. 3942-3948.
24. Saïd-Sadier, N. and D.M. Ojcius, *Alarmins, Inflammasomes and Immunity.* Biomedical journal, 2012. **35**(6): p. 437-449.
25. Mariathasan, S., et al., *Cryopyrin activates the inflammasome in response to toxins and ATP.* Nature, 2006. **440**(7081): p. 228-232.
26. Halle, A., et al., *The NALP3 inflammasome is involved in the innate immune response to amyloid-* β. Nature immunology, 2008. **9**(8): p. 857-865.
27. Duncan, J.A., et al., *Neisseria gonorrhoeae activates the proteinase Cathepsin B to mediate the signaling activities of the NLRP3 and ASC - containing inflammasome.* Journal of immunology (Baltimore, Md. : 1950), 2009. **182**(10): p. 6460-6469.
28. Martinon, F., et al., *Gout-associated uric acid crystals activate the NALP3 inflammasome.* Nature, 2006. **440**(7081): p. 237-241.
29. Shimada, K., T.R. Crother, and M. Arditi, *Innate immune responses to Chlamydia pneumoniae infection: Role of TLRs, NLRs, and the Inflammasome.* Microbes and infection / Institut Pasteur, 2012. **14**(14): p. 1301-1307.
30. Moayeri, M., I. Sastalla, and S.H. Leppla, *Anthrax and the inflammasome.* Microbes and Infection / Institut Pasteur, 2012. **14**(5): p. 392-400.
31. Ciraci, C., et al., *Control of innate and adaptive immunity by the inflammasome.* Microbes and infection / Institut Pasteur, 2012. **14**(14): p. 1263-1270.
32. Martinon, F., A. Mayor, and J. Tschopp, *The Inflammasomes: Guardians of the Body.* Annual Review of Immunology, 2009. **27**(1): p. 229-265.
33. Sutterwala, F.S., et al., *Critical Role for NALP3/CIAS1/Cryopyrin in Innate and Adaptive Immunity through Its Regulation of Caspase-1.* Immunity, 2006. **24**(3): p. 317-327.
34. Gross, O., et al., *Syk kinase signalling couples to the Nlrp3 inflammasome for anti-fungal host defence.* Nature, 2009. **459**(7245): p. 433-436.
35. Tiemi Shio, M., et al., *Malarial Hemozoin Activates the NLRP3 Inflammasome through Lyn and Syk Kinases.* PLoS Pathog, 2009. **5**(8): p. e1000559.

36. SaÔd-Sadier, N., et al., *<italic>Aspergillus fumigatus</italic> Stimulates the NLRP3 Inflammasome through a Pathway Requiring ROS Production and the Syk Tyrosine Kinase.* PLoS ONE, 2010. **5**(4): p. e10008.
37. Kayagaki, N., et al., *Non-canonical inflammasome activation targets caspase-11.* Nature, 2011. **479**(7371): p. 117-121.
38. Kayagaki, N., et al., *Noncanonical Inflammasome Activation by Intracellular LPS Independent of TLR4.* Science, 2013. **341**(6151): p. 1246-1249.
39. Kayagaki, N., et al., *Caspase-11 cleaves gasdermin D for non-canonical inflammasome signalling.* Nature, 2015. **526**(7575): p. 666-671.
40. Haggerty, C.L., et al., *Risk of Sequelae after Chlamydia trachomatis Genital Infection in Women.* Journal of Infectious Diseases, 2010. **201**(Supplement 2): p. S134-S155.
41. Genc, M. and P.-A. Mardh, *A Cost-effectiveness Analysis of Screening and Treatment for Chlamydia trachomatis Infection in Asymptomatic Women.* Annals of Internal Medicine, 1996. **124**(1_Part_1): p. 1-7.
42. Taylor, B.D. and C.L. Haggerty, *Management of Chlamydia trachomatis genital tract infection: screening and treatment challenges.* Infection and drug resistance, 2011. **4**: p. 19-29.
43. Morrison, R.P., K. Feilzer, and D.B. Tumas, *Gene knockout mice establish a primary protective role for major histocompatibility complex class II-restricted responses in Chlamydia trachomatis genital tract infection.* Infection and Immunity, 1995. **63**(12): p. 4661-4668.
44. Ito, J.I. and J.M. Lyons, *Role of Gamma Interferon in Controlling Murine Chlamydial Genital Tract Infection.* Infection and Immunity, 1999. **67**(10): p. 5518-5521.
45. Morrison, S.G. and R.P. Morrison, *Resolution of Secondary Chlamydia trachomatis Genital Tract Infection in Immune Mice with Depletion of Both CD4(+) and CD8(+) T cells.* Infection and Immunity, 2001. **69**(4): p. 2643-2649.
46. Morrison, S.G., et al., *Immunity to Murine Chlamydia trachomatis Genital Tract Reinfection Involves B Cells and CD4(+) T Cells but Not CD8(+) T Cells.* Infection and Immunity, 2000. **68**(12): p. 6979-6987.
47. Karunakaran, K.P., et al., *Development of a Chlamydia trachomatis T-cell vaccine.* Human Vaccines, 2010. **6**(8): p. 676-680.
48. Su, H., et al., *Chlamydia trachomatis genital tract infection of antibody-deficient gene knockout mice.* Infection and Immunity, 1997. **65**(6): p. 1993-1999.
49. Ramsey, K.H., L.S. Soderberg, and R.G. Rank, *Resolution of chlamydial genital infection in B-cell-deficient mice and immunity to reinfection.* Infection and Immunity, 1988. **56**(5): p. 1320-1325.
50. Zheng, J., et al., *Preparation and evaluation of monoclonal antibodies against chlamydial protease-like activity factor to detect Chlamydia pneumoniae antigen in early pediatric pneumonia.* European Journal of Clinical Microbiology & Infectious Diseases, 2015. **34**(7): p. 1319-1326.

51. Gurfinkel, E. and G. Bozovich, *Chlamydia pneumoniae: inflammation and instability of the atherosclerotic plaque.* Atherosclerosis. **140**: p. S31-S35.
52. Campbell, L.A. and C.-c. Kuo, *Chlamydia pneumoniae [mdash] an infectious risk factor for atherosclerosis?* Nat Rev Micro, 2004. **2**(1): p. 23-32.
53. Sessa, R., et al., *Chlamydia pneumoniae and atherosclerosis: current state and future prospectives.* International Journal of Immunopathology & Pharmacology, 2009. **22**(1): p. 9-14.
54. Wolf, K. and K.A. Fields, *Chlamydia pneumoniae impairs the innate immune response in infected epithelial cells by targeting TRAF3.* Journal of Immunology, 2013. **190**(4): p. 1695-701.
55. Vanrompay, D., R. Ducatelle, and F. Haesebrouck, *Chlamydia psittaci infections: a review with emphasis on avian chlamydiosis.* Veterinary Microbiology, 1995. **45**(2–3): p. 93-119.
56. Entrican, G., et al., *Cytokine release by ovine macrophages following infection with Chlamydia psittaci.* Clinical and Experimental Immunology, 1999. **117**(2): p. 309-315.
57. Moulder, J.W., *Interaction of chlamydiae and host cells in vitro.* Microbiological Reviews, 1991. **55**(1): p. 143-190.
58. Dautry-Varsat, A., A. Subtil, and T. Hackstadt, *Recent insights into the mechanisms of Chlamydia entry.* Cellular Microbiology, 2005. **7**(12): p. 1714-1722.
59. Hackstadt, T., et al., *Origins and functions of the chlamydial inclusion.* Trends in Microbiology. **5**(7): p. 288-293.
60. Wyrick, P.B., *Intracellular survival by Chlamydia.* Cellular Microbiology, 2000. **2**(4): p. 275-282.
61. Sellami, H., et al., *Chlamydia trachomatis infection increases the expression of inflammatory tumorigenic cytokines and chemokines as well as components of the Toll-like receptor and NF- κ B pathways in human prostate epithelial cells.* Molecular and Cellular Probes, 2014. **28**(4): p. 147-154.
62. Quayle, A.J., *The innate and early immune response to pathogen challenge in the female genital tract and the pivotal role of epithelial cells.* Journal of Reproductive Immunology. **57**(1): p. 61-79.
63. Rasmussen, S.J., et al., *Secretion of proinflammatory cytokines by epithelial cells in response to Chlamydia infection suggests a central role for epithelial cells in chlamydial pathogenesis.* Journal of Clinical Investigation, 1997. **99**(1): p. 77-87.
64. Kedersha, N.L. and L.H. Rome, *Preparative agarose gel electrophoresis for the purification of small organelles and particles.* Analytical Biochemistry, 1986. **156**(1): p. 161-170.
65. *Isolation and characterization of a novel ribonucleoprotein particle: large structures contain a single species of small RNA.* The Journal of Cell Biology, 1986. **103**(3): p. 699-709.

66. *Vaults. II. Ribonucleoprotein structures are highly conserved among higher and lower eukaryotes.* The Journal of Cell Biology, 1990. **110**(4): p. 895-901.
67. Kedersha, N.L. and L.H. Rome, *Isolation and characterization of a novel ribonucleoprotein particle: large structures contain a single species of small RNA.* The Journal of Cell Biology, 1986. **103**(3): p. 699-709.
68. Kickhoefer, V.A., et al., *Vaults and Telomerase Share a Common Subunit, TEP1.* Journal of Biological Chemistry, 1999. **274**(46): p. 32712-32717.
69. Harrington, L., et al., *A Mammalian Telomerase-Associated Protein.* Science, 1997. **275**(5302): p. 973-977.
70. Nakayama, J.-i., et al., *TLP1: A Gene Encoding a Protein Component of Mammalian Telomerase Is a Novel Member of WD Repeats Family.* Cell, 1997. **88**(6): p. 875-884.
71. Berger, W., et al., *Vaults and the major vault protein: Novel roles in signal pathway regulation and immunity.* Cellular and Molecular Life Sciences, 2008. **66**(1): p. 43-61.
72. Stephen, A.G., et al., *Assembly of Vault-like Particles in Insect Cells Expressing Only the Major Vault Protein.* Journal of Biological Chemistry, 2001. **276**(26): p. 23217-23220.
73. Poderycki, M.J., et al., *The Vault Exterior Shell is a Dynamic Structure that Allows Incorporation of Vault Associated Proteins into its Interior.* Biochemistry, 2006. **45**(39): p. 12184-12193.
74. Champion, C.I., et al., *A Vault Nanoparticle Vaccine Induces Protective Mucosal Immunity.* PLoS ONE, 2009. **4**(4): p. e5409.
75. Heinonen, P.K. and A. Miettinen, *Laparoscopic study on the microbiology and severity of acute pelvic inflammatory disease.* Eur J Obstet Gynecol Reprod Biol, 1994. **57**(2): p. 85-9.
76. Wiesenfeld, H.C., et al., *Comparison of Acute and Subclinical Pelvic Inflammatory Disease.* Sexually Transmitted Diseases, 2005. **32**(7): p. 400-405.
77. Kar, U.K., et al., *Vault Nanocapsules as Adjuvants Favor Cell-Mediated over Antibody-Mediated Immune Responses following Immunization of Mice.* PLoS ONE, 2012. **7**(7): p. e38553.
78. Buehler, D.C., et al., *Bioengineered Vaults: Self-Assembling Protein Shell–Lipophilic Core Nanoparticles for Drug Delivery.* ACS Nano, 2014. **8**(8): p. 7723-7732.
79. Zhu, Y., et al., *Activation of the NLRP3 inflammasome by vault nanoparticles expressing a chlamydial epitope.* Vaccine, 2015. **33**(2): p. 298-306.
80. Hoover, C.I. and E. Newbrun, *Survival of Bacteria from Human Dental Plaque Under Various Transport Conditions.* Journal of Clinical Microbiology, 1977. **6**(3): p. 212-218.
81. Thornberry, N.A., et al., *A Combinatorial Approach Defines Specificities of Members of the Caspase Family and Granzyme B: FUNCTIONAL RELATIONSHIPS ESTABLISHED FOR KEY MEDIATORS OF APOPTOSIS.* Journal of Biological Chemistry, 1997. **272**(29): p. 17907-17911.

82. Ng, G., et al., *Receptor-independent, direct membrane binding leads to cell surface lipid sorting and Syk kinase activation in dendritic cells.* Immunity, 2008. **29**(5): p. 807-818.
83. Xu, S., et al., *Activated Dectin-1 Localizes to Lipid Raft Microdomains for Signaling and Activation of Phagocytosis and Cytokine Production in Dendritic Cells.* The Journal of Biological Chemistry, 2009. **284**(33): p. 22005-22011.
84. Kowalski, M.P., et al., *Host Resistance to Lung Infection Mediated by Major Vault Protein in Epithelial Cells.* Science (New York, N.Y.), 2007. **317**(5834): p. 130-132.
85. Kickhoefer, V.A., et al., *Targeting Vault Nanoparticles to Specific Cell Surface Receptors.* ACS nano, 2009. **3**(1): p. 27-36.
86. Bui, F.Q., et al., *Fusobacterium nucleatum infection of gingival epithelial cells leads to NLRP3 inflammasome-dependent secretion of IL-1β and the danger signals ASC and HMGB1.* Cellular Microbiology, 2016. **18**(7): p. 970-981.
87. Lim, C., et al., *Chlamydia pneumoniae infection of monocytes in vitro stimulates innate and adaptive immune responses relevant to those in Alzheimer's disease.* Journal of Neuroinflammation, 2014. **11**: p. 217.
88. Thornberry, N.A., et al., *A novel heterodimeric cysteine protease is required for interleukin-1[beta]processing in monocytes.* Nature, 1992. **356**(6372): p. 768-774.
89. Dewhirst, F.E., et al., *The Human Oral Microbiome.* Journal of Bacteriology, 2010. **192**(19): p. 5002-5017.
90. Martinon, F. and J. Tschopp, *NLRs join TLRs as innate sensors of pathogens.* Trends in Immunology, 2005. **26**(8): p. 447-454.
91. Lopez-Castejon, G. and D. Brough, *Understanding the mechanism of IL-1β secretion.* Cytokine & Growth Factor Reviews, 2011. **22**(4): p. 189-195.
92. Cheeniyil, A., et al., *Shear stress upregulates IL-1β secretion by Chlamydia pneumoniae- infected monocytes.* Biotechnology and bioengineering, 2015. **112**(4): p. 838-842.
93. Ojcius, D.M., et al., *Apoptosis of epithelial cells and macrophages due to infection with the obligate intracellular pathogen Chlamydia psittaci.* J Immunol, 1998. **161**(8): p. 4220-6.
94. Rothermel, C.D., et al., *Chlamydia trachomatis-induced production of interleukin-1 by human monocytes.* Infect Immun, 1989. **57**(9): p. 2705-11.
95. Abdul-Sater, A.A., et al., *Inflammasome-dependent Caspase-1 Activation in Cervical Epithelial Cells Stimulates Growth of the Intracellular Pathogen Chlamydia trachomatis.* The Journal of Biological Chemistry, 2009. **284**(39): p. 26789-26796.
96. Itoh, R., et al., *Chlamydia pneumoniae harness host NLRP3 inflammasome-mediated caspase-1 activation for optimal intracellular growth in murine macrophages.* Biochemical and Biophysical Research Communications, 2014. **452**(3): p. 689-694.

97. Bui, F.Q., et al., *Fusobacterium nucleatum infection of gingival epithelial cells leads to NLRP3 inflammasome-dependent secretion of IL-1 β and the danger signals ASC and HMGB1.* Cellular Microbiology, 2016: p. n/a-n/a.
98. Kumar, M., et al., *Inflammasome Adaptor Protein Apoptosis-Associated Speck-Like Protein Containing CARD (ASC) Is Critical for the Immune Response and Survival in West Nile Virus Encephalitis.* Journal of Virology, 2013. **87**(7): p. 3655-3667.
99. Baroja-Mazo, A., et al., *The NLRP3 inflammasome is released as a particulate danger signal that amplifies the inflammatory response.* Nat Immunol, 2014. **15**(8): p. 738-48.
100. Franklin, B.S., et al., *The adaptor ASC has extracellular and 'prionoid' activities that propagate inflammation.* Nat Immunol, 2014. **15**(8): p. 727-37.
101. Li, X., et al., *Systemic Diseases Caused by Oral Infection.* Clinical Microbiology Reviews, 2000. **13**(4): p. 547-558.
102. Gurcel, L., et al., *Caspase-1 Activation of Lipid Metabolic Pathways in Response to Bacterial Pore-Forming Toxins Promotes Cell Survival.* Cell, 2006. **126**(6): p. 1135-1145.
103. Li, Y., et al., *Activation of Sterol Regulatory Element Binding Protein and NLRP3 Inflammasome in Atherosclerotic Lesion Development in Diabetic Pigs.* PLoS ONE, 2013. **8**(6): p. e67532.
104. Bartova, J., et al., *Periodontitis as a Risk Factor of Atherosclerosis.* Journal of Immunology Research, 2014. **2014**: p. 9.
105. Haynes, W.G. and C. Stanford, *Periodontal Disease and Atherosclerosis: From Dental to Arterial Plaque.* Arteriosclerosis, Thrombosis, and Vascular Biology, 2003. **23**(8): p. 1309-1311.